RF Hardware Design of a Stepped Frequency Continuous Wave Ground Penetrating Radar

Marten Kabutz

RF Hardware Design of a Stepped Frequency Continuous Wave Ground Penetrating Radar

by

Marten Kabutz

B.Sc(Eng) *Cape Town*

Submitted to the Department of Electrical Engineering
in partial fulfillment of the requirements for the degree of

MSc(Eng)

at the

UNIVERSITY OF CAPE TOWN

June 1995

Signature of Author.....
Department of Electrical Engineering
June 22, 1995

Certified by.....
Prof. M.R. Inggs
Director of the Radar Remote Sensing Group
Thesis Supervisor

Accepted by.....
Prof. Barry J. Downing
Head of Department

Declaration

I declare that this thesis is my own work. It is being submitted for the degree of Master of Science in Engineering at the University of Cape Town. It has not been submitted before for any degree or examination at this or any other university.

Marten Kabutz
June 22, 1995

Acknowledgments

Firstly, I would like to thank God, without whom this all probably never would have happened. Thanks also to my family for their support.

I am especially grateful for the supervision and support of Prof. Inggs. Many thanks to Prof. Inggs and Alan Langman for their technical input and expertise.

I would like thank Thomas Alsen for keeping me sane, Leon Alexander for keeping me fit, Alan Langman for keeping me working, Jasper Horrell for keeping me optimistic, Shaneen Gani for keeping me up to date, Greg Cox for keeping me humming and the rest of the UCT postgrads for their encouragement.

I am deeply indebted to Johnny Clegg, Peter Gabriel, Melissa Etheridge, Tony Cox and Metallica for helping me to keep going.

Finally, I would like to thank Alex.

Synopsis

Research into stepped frequency continuous wave ground penetrating radar (SFCW GPR) at UCT has been carried out since 1990. A first generation system comprising of Hewlett-Packard test equipment controlled by a PC was assembled. Cavity-backed log spiral antennas were designed and built by the University of Stellenbosch for the specific use of ground penetrating radar. Measurements with the first generation system proved the concept of SFCW GPR and thus a dedicated second generation system was planned.

A SFCW GPR system was designed to replace the first generation system. Various designs for transmitter and receiver configurations were investigated and those found most suitable were used for the implementation.

The SFCW radar consists of a wideband CW transmitter and a coherent receiver. A 300-1000 MHz transmitter was constructed using varactor-tuned oscillators as frequency sources. A double-sideband, low-IF receiver was constructed for the 300-1000 MHz signal, to mix it to an IF of 10.7 MHz and I-Q demodulate it. The transmitter was found to operate according to specifications. The receiver was found to operate satisfactorily, but the dynamic range was less than expected.

A limiting problem encountered in the first generation GPR was the large direct coupling signal from the transmitter into the receiver. This large signal reduced the effective receiver dynamic range. A method of cancelling this large direct coupling signal was implemented, using a bi-phase modulator to generate the cancelling signal in anti-phase to the coupling signal. A 20 dB reduction in coupling was shown.

The system was used to measure cable lengths to within the inherent accuracy of the system. A metal plate target was detected by the system feeding two antenna and a concrete floor was detected under 1 m of sand. It was thus shown that the SFCW system could be used as a second generation GPR.

Contents

List of Figures

List of Tables

Chapter 1

Introduction

1.1 Scope

This thesis describes the design and construction of a portable ground penetrating radar (GPR) using stepped frequency, UHF continuous waves. The scope of the thesis includes the design of a dedicated GPR2 system to replace and improve on the existing UCT GPR1 system. The first generation GPR1 system consists of Hewlett-Packard (HP) Test Equipment and a PC mounted in 2 shock-proof frames. The scope of the thesis further includes the construction of the GPR2 system from the antenna feed to the data acquisition. The scope of the thesis does not include the antennas in the front end, nor the signal processing in the final stages of the system.

1.2 Overview

The theory of a stepped frequency ground penetrating radar system is discussed in Chapter 2.1. First the basic theory of operation of a stepped frequency radar is discussed. Next, the limitations of the existing first generation equipment are shown. A comparison with a pulsed system is then provided to show the strengths and weaknesses of a SFCW system. The theoretical requirements for the transmitter are discussed, including the effects of unwanted phenomena like source frequency drift. The receiver requirements are listed. A short discussion on the necessity of a feedthrough cancella-

tion system is then provided. The feedthrough cancellation system is then discussed in detail in Chapter 5.

The transmitter is discussed in Chapter 3. The transmitter is the heart of a CW system, since the coherency of the transmit-receive signals determines the accuracy of the measurements. The primary requirements for a SFCW transmitter are wide bandwidth, good phase noise and a fast setting time. Some of the designs that can be used to achieve these criteria are:

- multiple oscillators to cover the complete bandwidth,
- one higher frequency oscillator mixed down to the desired band,
- phase locked loop design or
- a frequency synthesizer.

The system used for the SFCW was the 3 oscillator configuration in free running mode. The advantages of such a system are fast settling time, wide bandwidth and low cost. The disadvantages are that the stability and phase noise are not quite as good as desired.

The receiver system is discussed in Chapter 4. The limitation in dynamic range with and without feedthrough coupling and due to noise is shown. The noise figure for the SFCW radar is calculated and the effect of the positioning of the amplifiers and mixers is shown. Bandwidth considerations are then discussed since the receiver has to operate over a 300-1000 MHz bandwidth. The implementation of the receiver is discussed, starting with the low noise RF amplifier front end. Some of the output power is coupled from the transmitter and mixed with the IF. This signal is amplified to provide sufficient power to drive the receiver mixer. The receiver mixer thus has an RF receive input and an $RF \pm IF$ input and an IF output. This IF signal is filtered and amplified before being demodulated into in-phase and quadrature components. These measurements are sampled, converted to digital form and fed into a computer.

The problem of feedthrough cancellation is discussed in Chapter 5. An inherent problem with continuous wave systems is the large direct feedthrough signal from the transmit into the receive antenna. Conventional preventative techniques such as highly directional antennas and antenna separation cannot be used in GPR applications at UHF frequencies. A summary of possible techniques and specific problems to SFCW systems are discussed. The design for a practical feedthrough cancellation system is shown and the implementation described. Results using this feedthrough cancellation system are presented.

Results are presented in Chapter 6. Measurements of different cable lengths and of a metal plate being illuminated by two cavity-backed spiral antennas are shown. The system is shown to detect a concrete floor under a 1 m layer of sand.

Conclusions and recommendations on the next generation system are made in Chapter 7. The experience gained in this thesis is used to make recommendations on improvements to the Stepped Frequency Continuous Wave Radar System.

Chapter 2

System Design

The design of the radar system is shown in this chapter. First a brief basic theory section is given to introduce the principle of stepped frequency radar. The relative merits of pulsed and SFCW systems are then discussed and the SFCW radar is found to be more complex, but more versatile then the pulsed system. The first generation UCT GPR system is discussed. This comprised of conventional laboratory test equipment mounted in transportable containers. From the limitations of this radar, system parameters were gleaned to form the specifications of the portable radar system. From these the requirements on the transmitter, receiver and cancellation system were formulated.

2.1 Theory of Stepped Frequency Continuous Wave Radars

A stepped frequency continuous wave radar determines distance information from the phase shift in a target-reflected signal [15]. The reader is referred to a comprehensive treatment of the principle of SFCW radar by Iizuka et al [15] and Freundorfer[7]. Earlier work was done by Fowler et al [5]. A basic block diagram of a SFCW radar is shown in Figure 2-1. A signal generator generates a single frequency which is transmitted into a propagation medium. If there is some discontinuity in the dielectric property of the material, a fraction of the transmitted power will be reflected back. The block diagram shows the simple case of a plane target. An example of such an interface would be the water table under a few meters of sand. The received signal is then compared with the

transmitted signal and both the magnitude and phase measurements are taken. The complex frequency information is mapped into time by the Fast Fourier Transform and displayed.

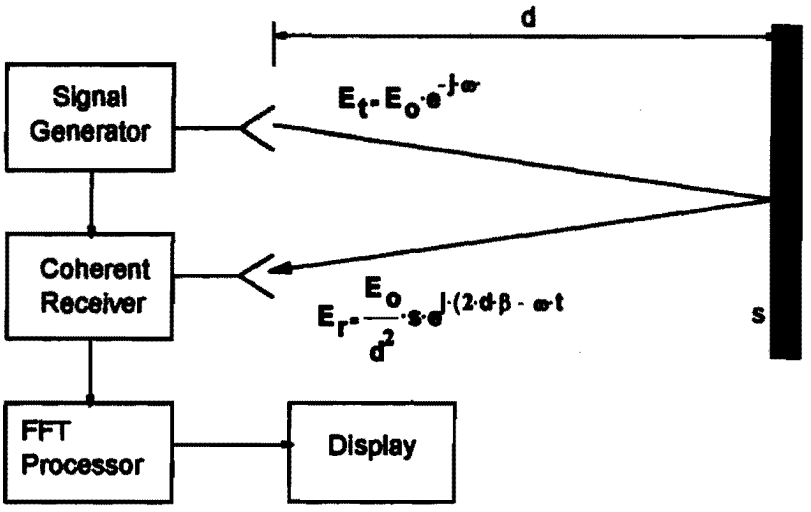

Figure 2-1: SFCW radar with a planar target

The transmitted signal $E_t e^{-jwt}$ is reflected by the target at a distance d. The interface has some complex reflection coefficient s. The received signal is thus:

$$E_r = s\frac{E_t}{d^2}e^{j(2\beta d - wt)} \tag{2.1}$$

where β is the propagation constant of the medium. If more targets are present, the reflections will add up in magnitude and phase. By stepping the frequency through N steps and taking the Fourier transform, the individual targets can be resolved. It has been shown [15], [7] that the range bin spacing Δz based on the Fourier series is:

$$\Delta z = \frac{c}{2\Delta f N\sqrt{\epsilon_r}} \tag{2.2}$$

where Δf is the frequency step

N is the total number of frequency steps

ϵ_r is the relative dielectric constant of the propagating medium

c is the speed of light in a vacuum

The corresponding unambiguous range of the stepped frequency radar in a medium is thus:

$$R_{unam} = (N-1)\Delta z \tag{2.3}$$

The required bandwidth to achieve this resolution and this unambiguous range is thus:

$$B = (N-1)\Delta f \tag{2.4}$$

It follows that if the lowest frequency of the bandwidth is f_o, the highest frequency will be $f_o + (N-1)\Delta f$.

2.2 Pulsed vs Stepped CW System

A comparison of a pulsed and a stepped frequency CW system shows that the main differences are found in the implementation. Pulsed radars measure the time taken for the transmitted pulse to return to the receiver. SFCW radars measure the frequency response and transform this into the time domain through a Discrete Fourier Transform or other transforms. The two techniques are thus equivalent through the Fourier Transform [7].

- **Antenna Considerations**

  In a pulsed system careful attention has to be given to the antennas, which have to be wide-band and non-dispersive. Multiple reflections inside the antennas are also a common problem.

  SFCW radars are coherent and the antenna criteria are far less stringent, since the frequency characteristics of the antennas can easily be normalized out with a reference measurement.

- **Antenna Feedthrough**

  Antenna feedthrough is the unwanted leakage from the transmit antenna into the receive antenna. Pulsed radars can easily deal with this problem by switching the receiver off while the transmitter is on.

Since SFCW radars operate with continuous frequencies, both transmitter and receiver have to be on during the measurement time. Thus complex external feedthrough cancellation techniques are necessary to reduce the coupling level.

- **System Complexity**

  In general, a SFCW radar system will always be more complex than an equivalent pulse system. An example of two such equivalent systems is given in [7]:

  > A typical pulsed radar system has a peak voltage of 1kV and a pulse width of 1.5ns. This is comparable to a SFCW radar with a bandwidth of 500 MHz, 64 frequency steps and an output power of 2 watts in a 50 Ω system. The actual equivalent parameters for the SFCW system described in this thesis are a peak voltage of 907V and an equivalent pulse width of 2 ns.

  The main components of a pulsed system are a high voltage pulse generator feeding the transmit antenna and a wide band receiver on the receive antenna. A SFCW system requires more complex receiver and transmitter circuitry - a stepped frequency transmitter and a coherent receiver with a narrow-band IF are necessary.

- **Processing**

  A SFCW radar system measures the complex frequency response by taking the in-phase and quadrature components of the received signal. These are transformed into a complex time domain response which in turn can be used to obtain the complex reflection coefficient from the target. Since a pulsed system is incoherent, only the real part of the received signal can be measured. The imaginary part of the signal can be obtained through the use of a Hilbert Transform. However, SFCW radar requires only one FFT to obtain the complex target reflection coefficient, whereas pulsed radar requires two FFT's to obtain the same information [7].

2.3 Description of First Generation System

The first generation SFCW radar system consisted of a Hewlett-Packard (HP) sweep frequency oscillator, an HP network analyzer, an RF power amplifier and a PC. A block diagram of the system is shown in Figure 2-2.

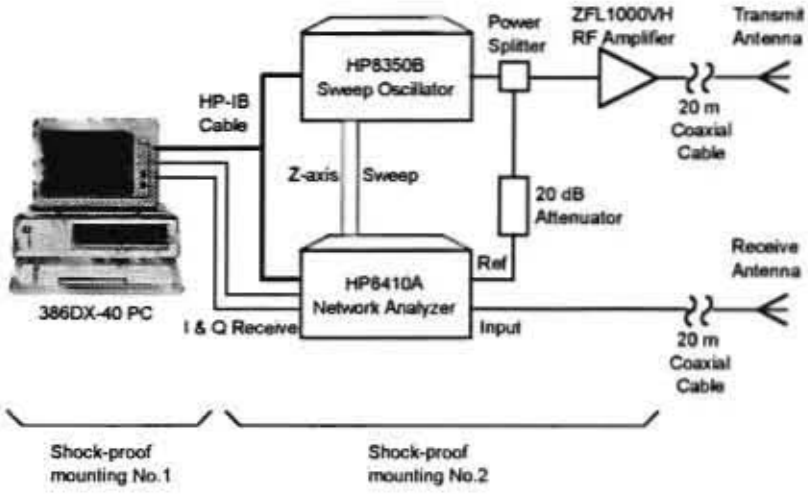

Figure 2-2: First Generation UCT SFCW GPR System

Since the HP Network Analyzer and the PC are sensitive to shock and vibrations, they had to be mounted into two shock-proof frames. Inside these frames, the system could be transported over rough terrain. However these frames had several disadvantages:

- The combined weight of the rugged shock proof mountings and the radar system was approximately 100kg and 130kg for the two boxes. This in turn led to portability problems. The radar system itself could not be transported away from a vehicle, so long antenna cable were necessary for measurement traverses. Measurements were only possible in areas accessible by motor vehicle.
- A motor vehicle or any other large metal object close to the measuring site could affect the measurements unless the antennas had an excellent front-to-back ratio.
- A 220 V AC generator was necessary to power the HP equipment and the PC.

Further drawbacks arising from the actual HP equipment were:

- The settling time of the signal generator was 300ms. This made measurements slow.
- A phase hysteresis in the network analyser made accurate phase measurements near 180° very difficult.

The second generation system should improve on these problems and these problems with the first generation system were incorporated into the system specifications.

2.4 System Specifications

The second generation stepped frequency continuous wave radar system should attempt to meet the following specifications which are justified in subsequent sections.

Bandwidth	300-1000 MHz
Frequency Resolution	2 MHz
Frequency Accuracy	10 kHz
Time per Scan	< 1 second per scan
Output Power	at least +20 dBm
Spectral Purity	< 60 dBc Harmonics and Spurii
Dynamic Range	60 dB
Cancellation Depth	20 dB
Weight	< 20 kg
Power	by rechargeable battery
Size	fitted onto antennas

Table 2.1: Transmitter Parameter Requirements

Each of these specifications generated specific requirements for the transmitter, receiver and cancellation circuits. Both the specifications and the system requirements are discussed in the subsequent sections.

2.5 Transmitter Requirements

2.5.1 Bandwidth

To achieve adequate resolution, a wide bandwidth is necessary for SFCW GPR (Section 2.1). The frequencies best suited for ground penetration are 100-1000 MHz [15], although the cut-off frequencies of this range can vary with soil type. Cavity-backed spiral antennas with a frequency range of 300-1000 MHz were available for the radar.

Since the antennas have a lower frequency cutoff of 300 MHz, the required transmitter bandwidth was limited to the range 300-1000 MHz. In soil with a dielectric constant $\epsilon_r = 4$, this 700 MHz bandwidth provides a resolution of:

$$d_r = \frac{c}{2B\sqrt{\epsilon_r}} = \frac{3 \cdot 10^8 \text{m/s}}{2 \cdot 700 \cdot 10^6 \text{Hz} \cdot \sqrt{4}} = 11\text{cm} \tag{2.5}$$

Often the resolution required does not make the full 700 MHz bandwidth necessary. The frequency range chosen for a specific application depends on the ground characteristics. For example, to achieve a resolution of 20cm in soil with $\epsilon_r = 16$, the required bandwidth is:

$$B = \frac{c}{2d_r\sqrt{\epsilon_r}} = \frac{3 \cdot 10^8 \text{m/s}}{2 \cdot 0.2\text{m} \cdot \sqrt{16}} = 188\text{MHz} \tag{2.6}$$

Thus although the full 700 MHz bandwidth will often not be used, the system was designed for a 700 MHz bandwidth to provide the possible application to a wide range of soil types and resolution requirements.

2.5.2 Frequency Resolution (Step Size)

The unambiguous range of the radar depends on the number of steps taken and the bandwidth used (Section 2.1). The resolution to which the frequency of the transmitter can be set thus determines how many steps can be taken in a bandwidth. Since a DFT has to be performed on the data, only powers of 2 (N=2^x) number of steps are generally taken. However, zero-padding can be used to extend any arbitrary number of frequency steps into a power of 2. The unambiguous range required for a specific application can be found by calculating at what range the return from a target in the lossy medium will no longer be visible.

For the above example of a bandwidth of 700 MHz, a dielectric constant of $\epsilon_r = 4$ and 128 steps, the unambiguous range R is:

$$R = \frac{c}{2B\sqrt{\epsilon_r}} \cdot (N-1) = \frac{3 \cdot 10^8 \text{m/s}}{2 \cdot 700 \cdot 10^6 \text{Hz} \cdot \sqrt{4}} \cdot 127 = 13.6\text{m} \tag{2.7}$$

An unambiguous range of this magnitude is sufficient of most ground penetrating ap-

plications. Using a minimum step size of 2 MHz and the maximum bandwidth of 700 MHz, an unambiguous range of 37 m will be obtained. This is sufficient even for optimum penetration depths (i.e. optimum soil types) and was thus chosen as a criteria for the transmitter.

2.5.3 Frequency Accuracy

A constant error in frequency over the measurement bandwidth does not degrade performance since the resolution and unambiguous range do not depend on the actual frequencies, but rather on the bandwidth and the step size. However, an error in the frequency step size will cause a limit in the dynamic range of the time domain plot after Fast Fourier Transform processing. The effect of step size error on the time domain plot was simulated by the following procedure: A gaussian distribution was used to model the frequency accuracy with a standard deviation equal to the frequency error. A single target was located exactly on a range bin thus fitting the Fourier series model for the ideal case. The time domain dynamic range was then found through an FFT. Successive iterations showed that a standard deviation of no more than 10 kHz was required for a 2 MHz step and a 60 dB dynamic range in the time domain.

2.5.4 Frequency Stability and Phase Noise

Frequency stability can be defined as the degree to which an oscillator produces the same frequency throughout a specified period of time [10]. The equation for a single frequency exhibiting phase noise and frequency instability is shown below in Equation 2.8:

$$V(t) = V_o(t)sin[\omega t + \Delta\phi_{fd}(t) + \Delta\phi_{pn}(t) + \Delta\phi_s(t)] \tag{2.8}$$

where V_o = nominal amplitude
ω = nominal frequency
$\Delta\phi_{fd}(t)$ = frequency drift (long term instability)
$\Delta\phi_{pn}(t)$ = phase noise (Short term instability)
$\Delta\phi_s(t)$ = spurious signals

The long term instability is the amount of frequency drift mostly due to temperature. This frequency change is too slow to have an effect on the frequency within one measurement time. Since the measurement of depth and the resolution do not depend on the actual frequencies used, but on the bandwidth and the number of steps, a gradual frequency drift is inconsequential for a SFCW application.

Most detrimental to the measurements is the frequency changes in the time that it takes for the wave to propagate to the target and back. The maximum penetration depth in ice can be as much as 300 m (Subsection 2.5.2). The phase propagation time for a target at a distance 300 m in air is $1\mu s$. The corresponding phase noise offset would thus be 1 MHz. The phase noise at this offset is generally well below -100 dBc [10] and should thus not effect the measurements in this way. For any ground probing applications, the maximum propagation distance will be well below 300 m.

The short term instability or phase noise is the amount of frequency change in within a measurement time. For a measurement time of 10 ms, the corresponding phase noise offset would be 100 Hz. The sources of random sideband noise include thermal noise, shot noise and flicker noise. This instability determines the minimum bandwidth that can be used in the IF stage and thus puts a limit on the possible noise performance of the system. The phase noise will thus limit the coherency, phase accuracy and bandwidth of the IF section.

2.5.5 Time per Scan

The radar has to step through N frequencies for a single scan. In order to make long traverses feasible, the time taken for each scan has to be minimized. The time per scan for the transmitter is the actual measurement time plus N times the settling time of the oscillator. The HP Oscillator used for the prototype system quoted a settling time of 300 ms. Thus a 300 ms wait-state had to be inserted for each frequency step before measurements could be taken. Thus for N=128 frequency steps, the total time lost due to oscillator settling is:

$$t_{scan} = 300ms \cdot 128 = 40s \tag{2.9}$$

If the settling time can be reduced to be minimal with respect to the measurement time, the total time per scan can be reduced to less then 2 seconds. The minimum

settling time chosen was 1 ms. This is easily obtainable with varactor, hyper-abrupt or YIG-tuned oscillators. A typical Varactor-tuned oscillator can be swept over the entire frequency range in less than $1\mu s$ [1].

2.5.6 Output Power

The choice of output power of the transmitter is a trade-off between achieving greater penetration and a better signal-to-noise ratio against the maximum direct feedthrough power into the receiver without desensitization. The maximum output power can be calculated by adding antenna feedthrough isolation to the maximum receiver input power. Any feedthrough cancellation would thus increase the maximum transmitter output power and thus the effective dynamic range of wanted signals.

The feedthrough isolation from the transmit into the receive antenna for cavity backed spiral antennas was measured to be 30 dB. For a maximum receiver input of -20 dBm and a cancellation of 10 dB, the maximum transmit power is 20 dBm.

2.5.7 Spectral Purity

The frequency spectrum of an ideal SFCW transmitter at any one frequency step consists of only that one frequency. However any real oscillator will have some spurious frequencies and harmonic frequencies in the output. Since the transmit signal is used to mix with the received signal in the receiver, any unwanted frequencies in the transmit signal will also be received.

The wide tuning bandwidth needed for a SFCW transmitter makes it extremely difficult to filter out all harmonics and spurii to the desired level. The effect of transmitting more than one frequency is that a phase error will be introduced. By setting the minimum difference between the carrier level and any unwanted frequencies to greater than the receiver dynamic range, this error source will be eliminated.

2.6 Receiver Requirements

2.6.1 Bandwidth

The RF section of the receiver has to cover the band 300-1000 MHz. Since the system can be calibrated, gain flatness over the entire bandwidth is not of primary importance. However large variations will cause a increase in the noise figure for those regions with less gain. This will cause a corresponding loss in dynamic range.

The IF bandwidth is limited by the frequency stability of the transmitter and the minimum system noise is limited by the IF bandwidth. The minimum IF bandwidth to cover transmitter instability should thus be used.

2.6.2 Dynamic Range

The dynamic range is the range of input signal levels that can be detected within noise floor and the 1 dB compression point of the receiver. The dynamic range of the HP8410 network analyzer was approximately 60 dB. The design criteria for the receiver was thus chosen to attempt to achieve the same 60 dB dynamic range or to improve on it.

2.7 Feedthrough Cancellation Requirements

Direct coupling between the transmit and receive antennas of continuous wave radars limits the dynamic range of the receiver by inserting a large unwanted signal into the receiver front-end. This coupling signal is typically 20 dB above the strongest target reflection.

Pulsed radar systems overcome this direct coupling problem by time-domain gating the receiver. Since the wanted signal is of the same frequency as the coupling, filters as in doppler radars cannot be used. Thus the only solution is to add some vector to the received signal which will cancel the large coupling feedthrough. Various techniques exist to cancel some of the coupling over narrow bandwidths, but modern components

can extend these techniques to allow cancellation over octave or greater bandwidths. Some of the techniques that will be discussed involve digital control of coupling reduction, cancellation at IF and RF sections and feedback techniques to take into account ageing of the antenna and other components.

The only requirement for the feedthrough cancellation system was in the cancellation depth that could be achieved with the circuit. The amount of cancellation that can be achieved depends on how accurately the cancellation vector can be controlled in amplitude and phase. The maximum cancellation (C) that can be obtained for a signal with a phase error, $\Delta\phi$ and an amplitude error, ΔV is given by Equation 2.10

$$C[dB] = 20 \log_{10}|1 - \Delta V e^{j\Delta\phi}|^{-1} \tag{2.10}$$

Thus a cancellation depth of 40 dB could be achieved with a cancellation circuit that can control the cancellation vector to within 0.05 dB in amplitude and 0.5° in phase.

Chapter 3

The Transmitter

The transmitter is the heart of a CW system, since the coherency of the transmit-receive signals determines the accuracy of the measurements. The primary requirements for a SFCW transmitter used in this application are wide bandwidth, good frequency accuracy, good phase noise and a fast settling time. Some of the designs that can be used to achieve these criteria are:

- Using multiple oscillators to cover the required bandwidth
- Using one higher frequency oscillator mixed down to the desired band.
- Using either of the above techniques in a phase locked loop design
- Using a frequency synthesizer

The system used for the SFCW was the multiple oscillator configuration in free running mode. The advantages of such a system include a fast settling time, wide bandwidth and low cost. The disadvantages are that the stability and phase noise are not quite as good as desired.

3.1 Transmitter Designs

3.1.1 3 Oscillator Design

Voltage-tuned oscillators at UHF frequencies are only available with a 40-50% bandwidth of the centre frequency. It is thus necessary to use 3 oscillators to cover the desired range from 300-1000 MHz. A transmitter design covering the range 300-1000 MHz is shown in Figure 3-1.

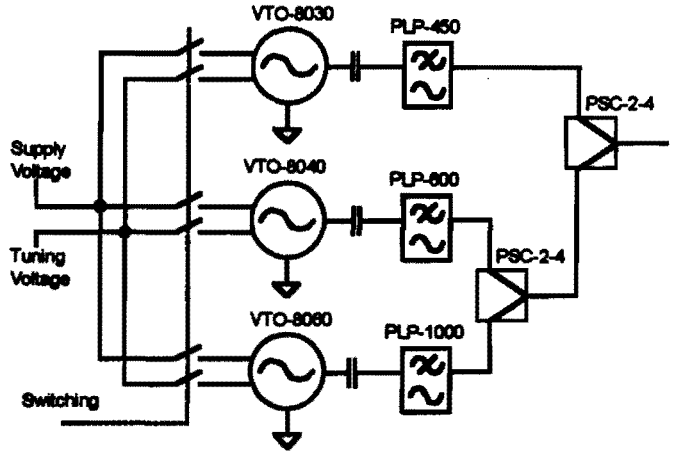

Figure 3-1: Transmitter using three UHF Oscillator

Three varactor-tuned oscillators are used to cover the frequency range 300-1000 MHz. The output of each oscillator is RF coupled to an appropriate filter to reduce the harmonic level. The three signals are combined with two power combiners.

Generating the frequencies with oscillators at the wanted frequencies rather than transmitter designs that use higher frequencies or synthesizers has the following advantages:

- no mixer products
- only known spurii from the oscillator
- each oscillator can be filtered individually

However it does have the disadvantage that multiple oscillators are needed to cover the frequency range with the associated switching circuits. The desired oscillator can be selected either by switching the supply voltage or by switching the RF signals.

Switching the supply voltage of the oscillators has the advantage that only one oscillator is running at any one time, preventing leakage from the other 2 oscillators into the transmit path. Most oscillators require a warm-up time during which they exhibit the most frequency drift. A switched supply system has the disadvantage that before and in between scans, all VCOs must be driven in order to keep them at operating temperature.

Switching the RF has the advantage that all 3 oscillators are at operating temperature where frequency drift will be minimal. However, RF switches are costly and provide an attenuation of approximately 40 dB. Thus some signal would be fed from the 2 unwanted oscillators into the transmit path.

Harmonics and spurious responses degrade the system performance and the optimal solution would be to implement a narrow band-pass tracking filter. The bandwidth of the filter should be as narrow as possible traded off against tracking speed. However, the filter would have to operate over the entire 300-1000 MHz bandwidth. This range could be split up into various parallel tracking filters, but the expensive and complexity of such a filtering system is beyond the scope of the project.

Spurious frequencies inside the tuning range cannot be filtered out, since any non-tracking filters would interfere with the desired signal. The oscillators thus have to be chosen to have an acceptable spurious level. Harmonics from frequencies below 500 MHz fall into the desired frequency range. These can only be filtered out by having a filter for each oscillator before the signals are combined. Since the oscillators operate over less than an octave bandwidth, sufficient attenuation at the harmonic frequencies can be obtained with a low-pass filter.

3.1.2 Single Oscillator Design

A single higher frequency oscillator with at least 700 MHz bandwidth can be mixed down to give a 300-1000 MHz output frequency range in a single sweep. Such a design can be seen in Figure 3-2.

In this design, the VTO-8150 which has a frequency range of 1.5-2.2 GHz is mixed down with a frequency of 1.2 GHz to provide a frequency range from 300-1000 MHz. The local oscillator frequency can also be used in the receiver to mix the received signal up to a 1.4 GHz IF frequency. Since the bandwidth of the VTO-8150 can be tuned over

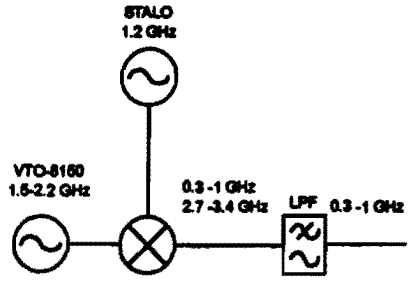

Figure 3-2: Transmitter using a Single L-Band Oscillator mixed down to UHF frequencies

1 GHz bandwidth, the above design can be easily be modified to provide an output frequency range of 100-1000 MHz.

Such a system would not require the switching circuit of a multi-oscillator approach. It would also simplify the control and tuning. However, a more stable tuning voltage would be required to obtain 2 MHz step sizes.

The second harmonic of the L-band oscillator is at 3 GHz. When this is mixed down with the 1.4 GHz LO, the resulting frequencies fall well outside the desired frequency range. Thus a single 1 GHz low-pass filter after the mixer is sufficient to filter out all the harmonics.

The major disadvantage of this single oscillator approach is the mixer in the transmit path. Any unwanted mixer products that fall into the wanted bandwidth cannot be filtered out.

3.1.3 Phase-locked Loop Design

Phase-locking the transmitter has the advantage of eliminating long term frequency drift and tuning without the need of a linearizer. A phase locked design could be used in both the 3 oscillator and the single oscillator design. Figure 3-3 shows a PLL implementation using the VTO-8030 varactor-tuned oscillator.

This design shows a VTO-8030 oscillator locked to a 1 MHz reference. The output of the oscillator has to be divided by 300-400 in 1 MHz steps to set the desired frequency. The frequency and phase difference between the divided signal and the reference is seen at the output of the phase detector. A double-balanced mixer can be used to perform

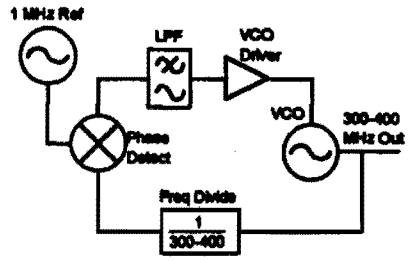

Figure 3-3: Transmitter showing one of the 3 Phase-Locked Loops

this function provided that both RF and LO inputs are driven at the same level. This output is low-pass filtered to provide loop stability and then used to tune the VCO through a voltage driver.

Some advantages of a PLL design include:

- long term frequency drift is eliminated
- exact tuning curve of VCOs does not have to be known

Some disadvantages of a PLL design:

- added complexity and cost
- no improvement in phase noise
- added lock-on time
- difficulty of keeping lock over such a wide bandwidth

The disadvantages of the PLL design can thus be seen to be severe, whereas the advantages are not significant for this stepped frequency radar application.

3.1.4 Frequency Synthesizer Design

A frequency synthesizer is the ideal SFCW transmitter in terms of frequency stability and reproducibility. The frequency can be made highly stable and accurate at the cost of increasing complexity. This design has been widely used in stepped frequency radar applications. Iizuka et al [15] and Uratsuka et al [25] used a two synthesizer system, where one synthesizer was used in the transmitter and another to follow the transmit signal offset by the IF. The block diagram of the system used by Uratsuka [25] is shown in Figure 3-4.

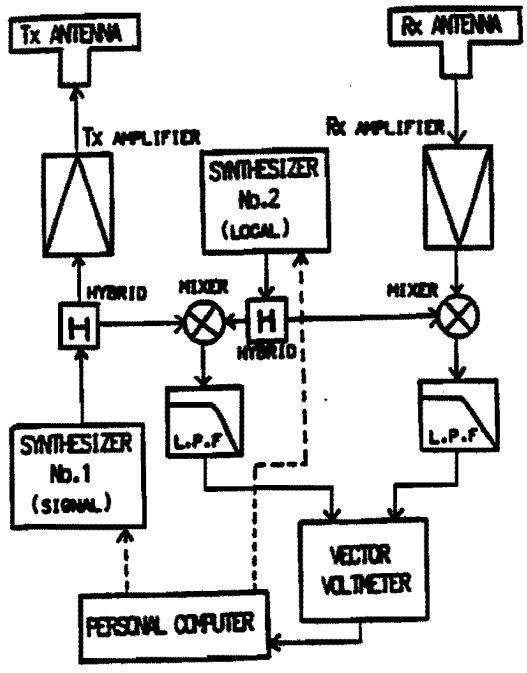

Figure 3-4: Block diagram of Step-Frequency Radar System used by Uratsuka et al

In this step frequency radar system, a frequency synthesizer, controlled by a PC, is used as a transmitter and another synthesizer is used to generate a replica of the transmit frequency offset by the IF. This signal is used in the receiver.

A frequency synthesizer is too costly and complex for this project and was mentioned here for completeness.

3.2 Hardware Design

The three-oscillator design shown in Figure 3-5 was used for the transmitter. It consists of 3 varactor tuned oscillators covering the range from 300-1000 MHz switched through the power supply. The outputs of these oscillators are individually filtered and then combined into one transmit output.

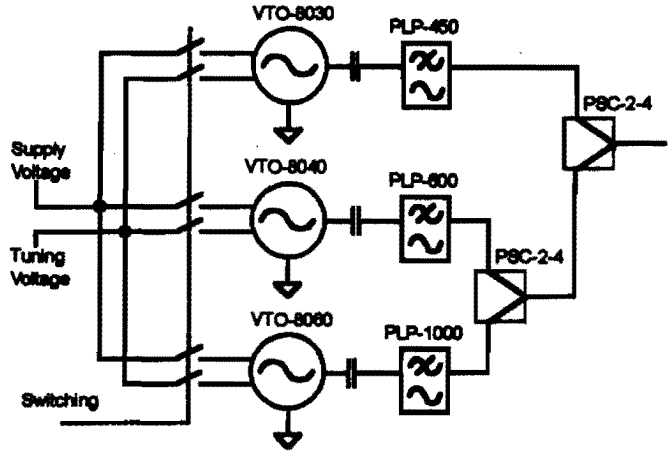

Figure 3-5: Transmitter using three UHF Oscillator

This design was chosen for the following reasons:

- Varactor-tuned oscillators to cover this range were readily available. These oscillators had the required bandwidth, low phase noise, low spurious level and a medium output power.
- The harmonics can easily be filtered out by using dedicated filters for each VCO.
- The output does not have any mixer products.

A single oscillator approach was not used because of the unwanted mixer products in the output. The phase-locked loop approach was not used since the benefits of less frequency drift and simpler tuning were outweighed by the added complexity, cost and potential instability of such a system. The implementation of a frequency synthesizer was beyond the scope of the project because of cost and complexity.

3.2.1 Oscillators

To obtain the 300-1000 MHz bandwidth, 3 varactor-tuned Avantek oscillators were used. These oscillators are tuned by varying the voltage across a varactor diode. The varactor diode thus acts as a voltage-variable capacitor in a microstripline resonator. The oscillators have an extremely fast tuning speed which is limited mainly by the output impedance of the tuning voltage driver. The measured parameters are shown in Table 3.1.

Model Number	VTO-8030	VTO-8040	VTO-8030
Frequency Range GHz	300-400 MHz	400-600 MHz	600-1000 MHz
Power Output into 50Ω	+11 dBm	+13 dBm	+13 dBm
Power Output Variation	±1 dB	±1 dB	±1 dB
Tuning Voltage @ Low Freq.	2.5 V	2.5 V	2.1 V
Tuning Voltage @ High Freq.	23.7 V	47.7 V	42.0 V
All Harmonics	-20 dBc	-19 dBc	-17 dBc
Spurious Output	-65 dBc	-62 dBc	-61 dBc
Phase noise 50kHz from carrier	-114 dBc/Hz	-114 dBc/Hz	-110 dBc/Hz

Table 3.1: Varactor-tuned Oscillator Specifications

The actual frequency ranges that these oscillators could be tuned to typically extended 10% below the low frequency limits shown above. The tuning voltages are the actual voltages required to achieve the low and high frequency limits shown. The harmonic levels are quite high and thus need to be filtered. The spurious levels are at least 60 dB below the carrier which is acceptable. The phase noise according to specification is very low. These exact measurements could not be confirmed due to lack of noise performance equipment.

All three VCOs had markedly different tuning curves. The tuning curve of the VTO-8030, shown in Figure 3-6, has a relatively constant slope making it possible to step the frequency with a low number of bits in the D/A which generates the control voltage from a PC. The exact number of bits required are calculated in Subsection 3.2.2.

The VTO-8040 tuning curve, seen in Figure 3-7, has a much greater variation in slope. This means that a larger number of bits are required to step the frequency accurately over this range.

The VTO-8060 tuning curve is shown in Figure 3-8. The slope of the tuning curve can

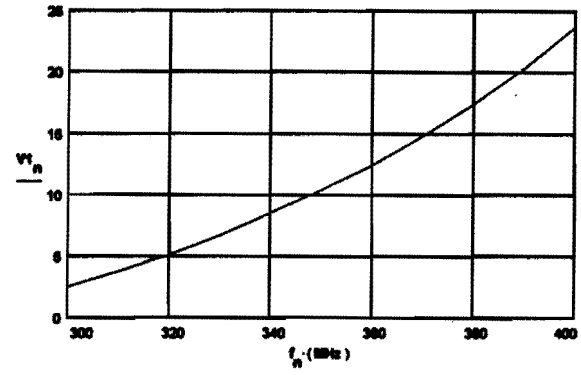

Figure 3-6: VTO-8030 Tuning Curve

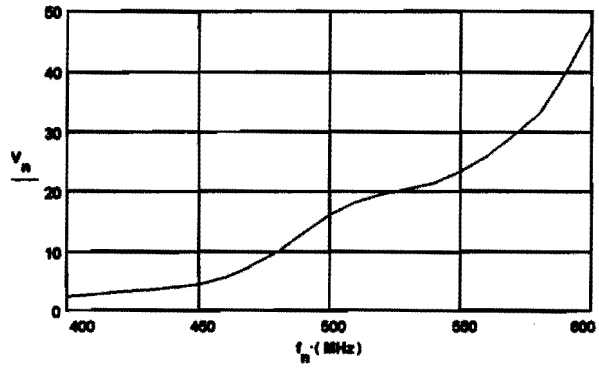

Figure 3-7: VTO-8040 Tuning Curve

also be seen to vary significantly. At this higher frequency, the curve is a great deal less smooth than the VTO-8030 tuning curve.

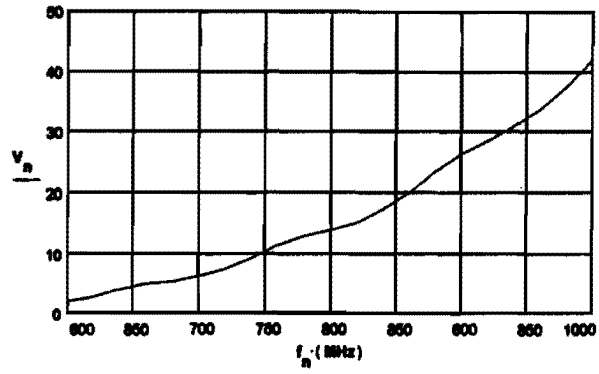

Figure 3-8: VTO-8060 Tuning Curve

3.2.2 Oscillator Tuning Circuit

The varactor-tuned oscillator require a driving voltage range of +2V to +45V. Since the voltage is controlled from a D/A, the 0-5V level has to be translated to 2-50V. The circuit shown in Figure 3-9 was used to do this level translation.

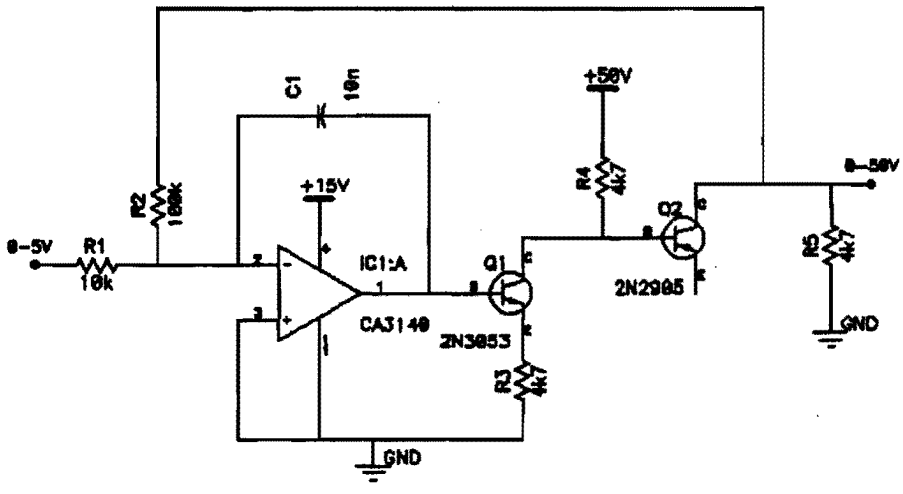

Figure 3-9: Tuning Circuit

The resistor R2 provides the feedback path and the gain of the circuit is thus R2/R1. The opamp CA3140 was chosen because it can be operate from a single supply. Thus only a +15V and a +50V supply is needed. Q1 and Q2 are complimentary NPN and PNP high voltage transistors that can be operated at up to 60V.

The number of bits required in the D/A can be calculated by using the flattest slope of the tuning voltages for the three oscillators. The flattest slope of the three tuning curves is at the low frequency end (approximately at 400 MHz) of the VTO-8040 oscillator. The tuning slope at this point is 29 mV/MHz. Thus the control voltage has to be adjustable to 58 mV to facilitate 2 MHz steps in this region. The voltage per bit for a 50 V tuning signal for different numbers of bits is:

$$\delta V = \frac{50}{2^N - 1}[V] \tag{3.1}$$

where dV is the voltage per bit and N is the number of bits. Thus at least 12 bits (which give a dV of 12.2 mV) are required. This would result in a maximum frequency error of 200 kHz (or 10%) due to quantization.

3.2.3 Switching Circuit

The 3 oscillators were switched by controlling the supply voltage rather than by RF switches. This method was used because of the advantage of eliminating all feedthrough from the unwanted oscillators and the lower cost. The transmitter would therefore need a warm-up time and the ability to have all three oscillators running together.

The 3 oscillators have to be switched with TTL logic in order to be PC-controllable. Since the following transmitter states have to be possible, 3 logic lines are needed to control the oscillators.

- All oscillators OFF
- Any one oscillator ON
- All oscillators ON

Analogue switches could not be used to switch the supply and control voltages because the supply draws 50 mA and the control can be as high as 50 V. Both these values exceed the specifications for the available analogue switches. Thus transistor driven reed relays were used. The circuit is shown in Figure 3-10.

This circuit was used to in triplicate to switch the three VCOs. The IC transistor package CA3081 containing 6 NPN transistors was used. R1 limits the current into the transistor base and C7 is a decoupling cap situated close to the transistor to prevent RF

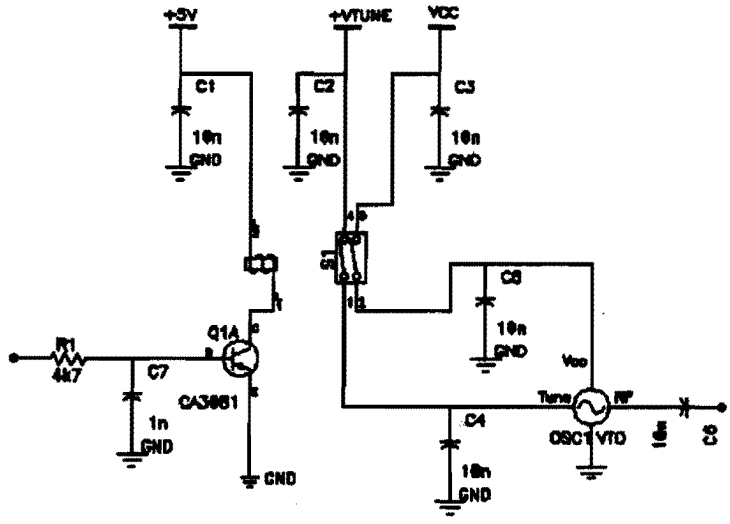

Figure 3-10: Switching Circuit

feedthrough. Switching the voltage at the base causes a 5V drop across the 140Ω coil. This switches both the tuning and supply voltage to the VCO. Decoupling capacitors were used close to the entry point onto the PCB and again close to the VCO. The RF output was RF-coupled through a 10 nF surface-mount capacitor.

3.2.4 Filters and Power Combiners

The following Mini-Circuits low-pass filters were used to reduce the harmonic levels of the oscillator outputs:

Model Number	PLP-450	PLP-600	PLP-1000
Corresponding Oscillator	VTO-8030	VTO-8040	VTO-8060
Passband (loss<1dB)	DC-400 MHz	DC-580 MHz	DC-900 MHz
Cutoff Frequency (loss=3dB)	440 MHz	640 MHz	990 MHz
Required Bandwidth	300-400 MHz	400-600 MHz	600-1000 MHz
Stopband MHz (loss>20dB)	580-750	840-1120	1340-1750
Stopband MHz (loss>40dB)	750-1800	1120-2000	1750-2000
2nd Harmonic MHz	600-800	800-1200	1200-2000
VSWR in Passband (Typ)	1.7:1	1.7:1	1.7:1
VSWR in Stopband (Typ)	18:1	18:1	18:1

Table 3.2: Low pass filter specifications

The required bandwidths for the three VCOs can be seen to fall below the 3 dB cut-off

frequency except in the case of the VTO-8060 VCO, where the last 10 MHz experience a loss of more than 3 dB. The 2nd harmonics are seen to be attenuated by at least 20 dB over most of the frequency range.

Since the output power level of the VTO-8030 VCO was approximately 3dB below the level of the other two VCOs, the signals from the VTO-8040 and the VTO-8060 were combined first. This provided an output power flatness of about 3dB over the entire tuning range. Although this flatness is not a requirement since calibration will provide a reference signal, it simplifies the receiver design and performance.

The high VSWR in the stopband of the filter means that the harmonics and spurii that fall into the stopband are reflected back into the oscillator. This is not desirable since it can affect the performance of the oscillator. The solution would be to insert a 6dB attenuator between the oscillator and the filter. This would provide a 12dB return loss to the reflections. However, this problem was only found after construction of the transmitter and thus not rectified. The oscillators were observed to operate satisfactorily without the attenuator.

3.2.5 Board Layout

The printed circuit board layout for the RF section of the transmitter is shown in Figure 3-11. Decoupling capacitors can be seen at both the supply and tuning voltage inputs to each of the oscillators. From the RF output pin of each oscillator, a 50Ω microstrip line feeds into a 1 nF surface-mount feedthrough capacitor (not shown). Then follows the appropriate Mini-Circuits low-pass filter for each oscillator. The filtered VTO-8040 and VTO-8060 outputs are combined and then combined with the filtered VTO-8030 output. The microstrip bends were designed with Touchstone to give a flat frequency response.

Most of the unused space on the track-side of the board was covered with copper conductor, leaving enough space (100 mils) to minimize coupling to the microstrip lines. The component side of the board was one continuous ground plane and joined to the top ground plane by numerous through connections (not shown in Figure 3-11).

The layout of the switching circuit is not as critical as that of the RF section. Ground planes and decoupling capacitors were used to minimize RF contamination of these signals. A +5V regulator was used to generate the +5V supply required for the transistor

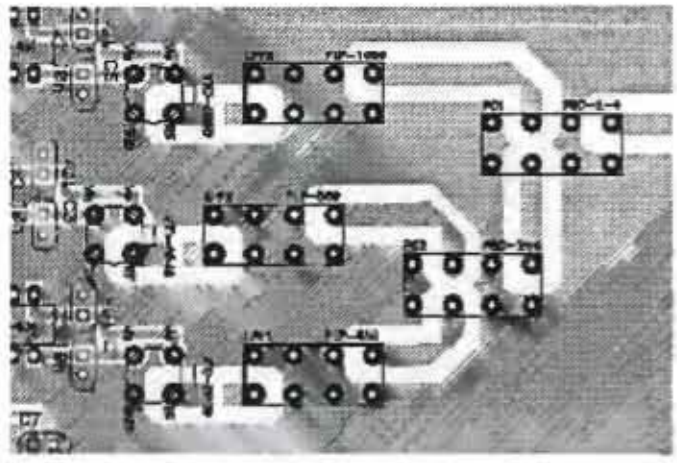

Figure 3-11: RF section of the transmitter board

switches and the reed relays. This was done so that only the following input signals and voltages are necessary:

- +15V Supply (200 mA)
- 0-50V Tuning Signal ($\sim 1\mu A$)
- 3 Digital switching lines

There is a single 50Ω BNC connector for the RF output of the transmitter. A photograph of the complete transmitter is shown in Figure 3-12.

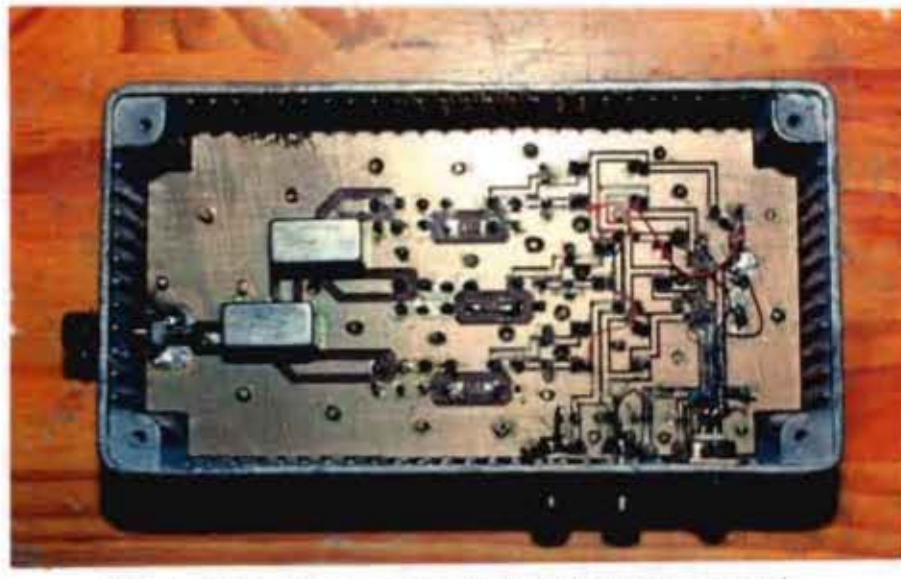

Figure 3-12: Photograph of the transmitter board

3.3 Transmitter Performance

The performance of the transmitter was evaluated with a spectrum analyzer. The spectral purity was observed by sweeping the transmitter over the entire range and observing the maximum harmonic and spurious levels. The phase noise was measured by directly viewing the signal over a narrow bandwidth. Phase jitter was found to be present in the varactor tuned oscillators.

3.3.1 Spectral Purity

The level of harmonics and spurii at the output of transmitter where observed on a spectrum analyzer. A typical frequency spectrum showing the harmonic levels is in Figure 3-13.

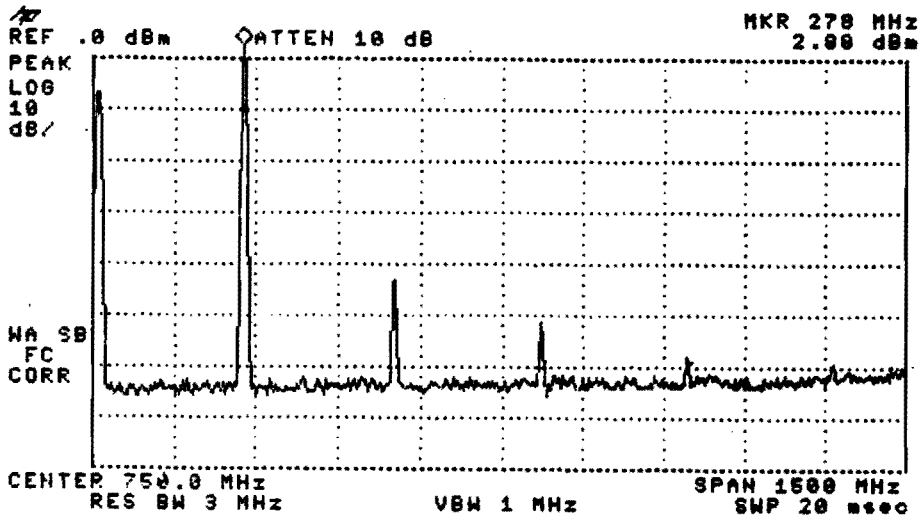

Figure 3-13: Frequency Spectrum of transmitted signal

The second harmonic is 45 dB below the carrier, the third harmonic is 57 dBc and the fourth harmonic is 61 dBc. No spurious responses can be seen for this particular frequency. Over the frequency range, harmonics were observed to be at least 40 dB below the carrier and spurii were seen to be at least 60 dB below the carrier.

3.3.2 Phase Noise

The only available method of measuring the phase noise of the transmitter was by measuring the phase noise directly with a spectrum analyzer. This method is only useful to get an approximate indication of the VCO phase noise. The equipment for accurate phase noise measurement was not available.

The output of the VTO-8030 VCO was observed for a single spectrum analyzer sweep as shown in Figure 3-14.

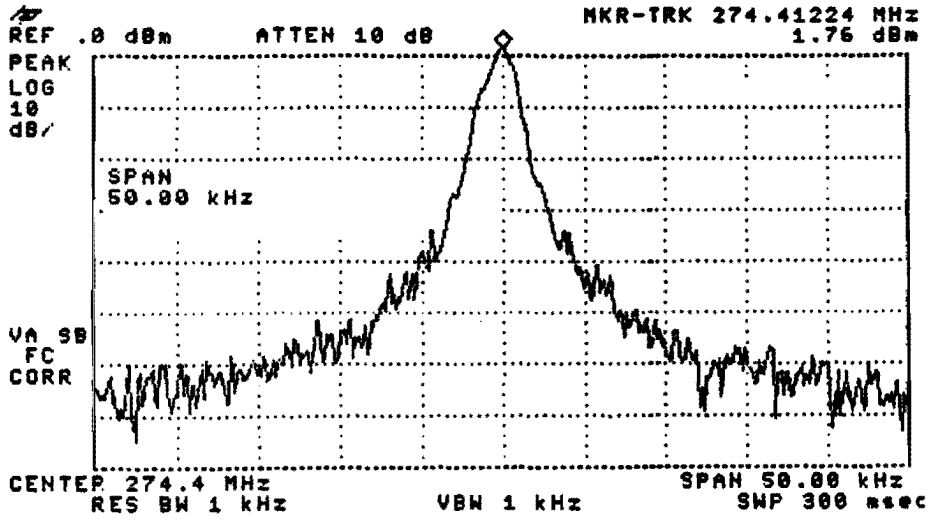

Figure 3-14: Spectrum Analyzer phase noise measurement (BW = 50 kHz)

The phase noise within 10 kHz of the signal can be seen in this plot. Further out, the measurement is contaminated by system noise, with is generated in the spectrum analyzer. The same frequency was then observed over a 20 kHz bandwidth and the display was averaged 100 times. The phase noise plot is shown in Figure 3-15:

A phase noise level of -60 dBc at 10 kHz offset can be seen in this plot. Phase noise cannot be measured at any larger frequency offsets since the noise floor of the spectrum analyzer is at -70 dBm.

3.3.3 Frequency Jitter

An unwanted phenomena that was observed was a frequency jitter on the transmit frequency. Figure 3-16 shows the bandwidth over which the frequency jitters.

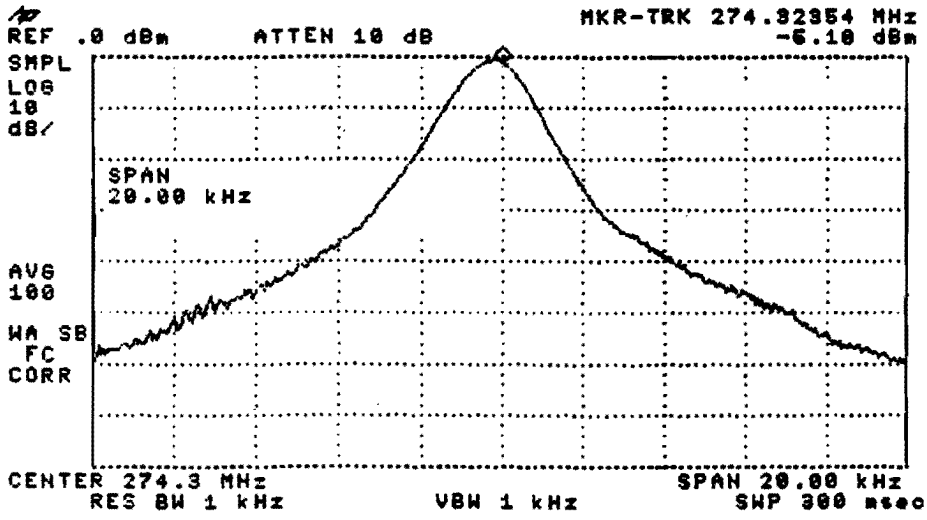

Figure 3-15: Spectrum Analyzer phase noise measurement (BW=20 kHz)

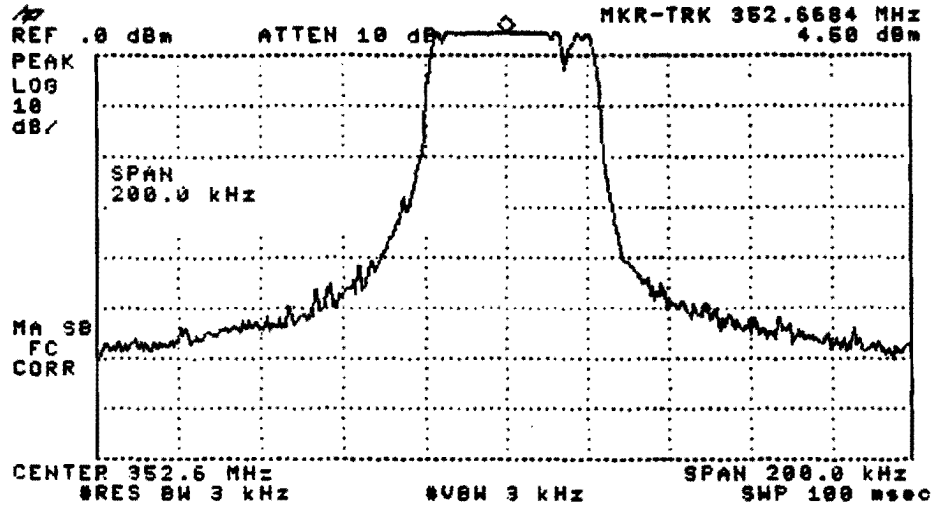

Figure 3-16: Frequency jitter of the transmitter

In order to show this frequency jitter, the spectrum analyzer was set to hold the maximum signal. The signal was allowed too add up over several seconds to obtain the extremities of the frequency jitter. The signal was seen to jump around erratically within the 40 kHz bandwidth seen above. Since this bandwidth is only 0.01% of the center frequency, the effect of this phenomena can be taken to be negligible. At the low frequency end of the oscillators, this 40 kHz jitter translated to a 0.8 mV RMS noise on the tuning voltage. Possible noise sources include the D/A converter and the level shifting circuit.

3.3.4 Frequency Accuracy

The frequency accuracy was seen to be dependant on two main factor: firstly the error due to the limited voltage step available by the 12-bit D/A and secondly thermal drift of the VCOs. The error due to the limited step size was measured have a standard deviation of 80 kHz. The thermal drift error could be separated into 2 components: a constant error in frequency to the entire range and the deviation at each frequency step on top of this constant. The constant offset was measured to drift by up to 200 kHz once the VCOs had been allowed to warm up. The standard deviation on top of this offset given the initial step size error was measured to be a maximum of 20 kHz.

The constant error due to the thermal effect does not degrade performance, since the resolution and unambiguous range do not depend on the actual frequencies, but rather on the bandwidth and the step size. The effective maximum frequency step error can thus be calculated by adding the error due to the D/A quantization to the deviation of the thermal offset. The accuracy of the frequency is thus to within 100 kHz. The dynamic range that can be achieved in the time domain through the FFT for a frequency step error of 100 kHz at 2 MHz steps was calculated to be 45 dB. Thus the frequency accuracy can be seen to below specifications.

Chapter 4

The Receiver

The SFCW receiver requires a multi-octave RF front-end which mixes down to a narrow band IF system. The flatness of the receiver frequency response over the entire bandwidth is not critical, since any deviations can be calibrated with a reference measurement. However, large variations in gain will affect the system noise performance and dynamic range. Four possible RF front-end designs are discussed:

- Single Low IF Receiver
- Receiver using the Single VCO Transmitter
- Receiver using a Higher and a Lower IF
- Frequency Synthesizer Receiver

The RF bandwidth from 300 to 1000 MHz has to be mixed to some IF at which it can be filtered. The IF signal must then be detected in quadrature so as to obtain the full signal information of the received frequency. Three methods of obtaining the in-phase and quadrature components of the received frequency are shown:

- Conventional I-Q Detection
- Switched I-Q Detection
- Sub-Nyquist Quadrature Sampling

Weighing up the relative merits of these designs resulted in a receiver design using a single low IF mixing system and conventional I-Q detection. The receiver block diagram and the receiver performance calculations demonstrate that this system can perform to specification. The RF and IF implementation is then documented in detail. Measurements of receiver performance follow.

4.1 Receiver Front-end Designs

The choice of intermediate frequency can be classified into three bands relative to the operating bandwidth B which extends from 300 MHz to 1 GHz:

- A *lower IF* can be used where $f_{LO} < 300$ MHz. In this case the sum and difference bands would always overlap and thus can not be separated. Both bands are thus present in the mixing signal.
- An *in-band IF* could be used where 300 MHz $< f_{LO} <$ 1 GHz. In this case the difference band would span DC and thus is of no use in the mixing signal. The sum band would thus have to be filtered and used exclusively. (The frequency separation between sum and difference is $2f_{LO} - 700$ MHz below 650 MHz and 600 MHz above 650 MHz.)
- A *higher IF* can be used where $f_{LO} >$ 1 GHz. Here either or both of the sum and difference bands can be used in the mixing signal. The frequency separation is a constant 600 MHz independent of f_{LO}.

Any one or combination of these IF frequencies can be chosen in the receiver. The sum and difference band considerations fall away in the case where the mixing signal is not generated by mixing f_{LO} by a reference of the transmitted signal.

4.1.1 Single and Double Sideband Systems

The receiver can be used as either a single- or double sideband system. In a single sideband configuration only one sideband of the mixing signal $f_{Tx} \pm f_{LO}$ is used. A double side-band system uses both $f_{Tx} + f_{LO}$ and $f_{Tx} - f_{LO}$ sidebands. The actual measurements that are taken with these two types of systems are markedly different.

The IF signal of a single-sideband system is shown below (from Appendix A.1):

$$V_{IF} = \frac{V_r}{2L_{mix}} sin(w_{IF}t - \theta_r + \theta_e) \tag{4.1}$$

where V_r and θ_r are the magnitude and the phase of the received signal, L_{mix} is the insertion loss of the mixer and θ_e is the phase error due to the reference signal path. Thus it can be seen that V_r and θ_r are modulated onto the magnitude and phase of the IF respectively. Detecting the IF in magnitude-phase or I-Q yields the complex signal information by which the time-domain plot can be obtained through the complex Fast Fourier transform.

The implementation of a single-sideband system involves the difficult task of rejecting one of the sidebands over a bandwidth of 700 MHz. At IF frequencies below 300 MHz, a single-sideband modulator could be used, but these are extremely difficult to construct over wide bandwidths. At IF frequencies of more than 650 MHz, the difference band could be rejected with a high pass filter. Thus a single-sideband system is only feasible for a first IF of 650 MHz or greater.

In a double-sideband system, both sidebands are used to drive the receiver mixer and the resultant IF signal can be shown (Appendix A.1) to be:

$$V_{IF} = \frac{V_r}{L_{mix}} cos(\theta_r - \theta_e) sin(w_{IF}t) \tag{4.2}$$

Thus both the magnitude and phase (V_r and θ_r) of the received signal are modulated onto the amplitude of the IF and there is no information in the IF phase. In addition, a 3 dB improvement in signal strength can be seen in the double-sideband system, since the sideband products are added. However, the average IF signal will remain the same because of the sinusoidal variation in amplitude. The IF signal can thus be detected in magnitude only. However the unambiguous range is halved through the real FFT.

The implementation of a double-sideband system does not involve any additional filtering as in the single-sideband case. The reference mixer output can be used to drive the receive mixer directly. However, the IF frequencies which can be used in this system are limited to outside the 300-1000 MHz bandwidth. Thus either a lower or higher IF would have to be used.

4.1.2 Single Low IF Receiver

A single IF stage at a frequency below the operating bandwidth can be used as a receiver system. An example of such a receiver with an IF of 10.7 MHz is shown in Figure 4-1. This receiver design could be used with any type of transmitter, since the only reference that is required is the transmit frequency.

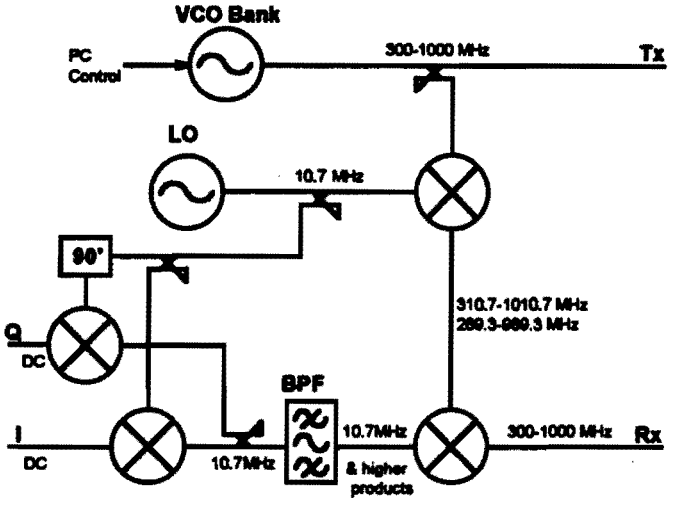

Figure 4-1: Receiver using a single low IF

A reference of the transmitted frequency is mixed with the local oscillator frequency f_{LO} ($< f_{min}$). This RF mixing signal is then used to drive the receiver mixer. Thus the received frequency f_{Rx} is mixed by $f_{Tx} \pm f_{LO}$, the transmit frequency offset by the IF frequency. The output of the receiver mixer will consist of the two difference terms added at the IF and the two sum terms which are rejected by the IF filter. The IF frequency is then detected by a quadrature detector.

The advantages of the system are the simplicity of the design and the ready availability of oscillators, narrow-band filters and I-Q detectors for the HF and UHF frequency range.

However, since the reference signal is mixed with the IF, unwanted mixer products will be present in the mixing signal. The wideband nature of the receiver makes it impossible to filter out any products in the pass band and these will mix with the received signal. This means that unwanted products will fall into the IF bandwidth and distort the I-Q measurements.

It is impossible to separate the sum and difference frequencies out of the RF mixing

signal ($f_{Tx} \pm f_{LO}$) because of the wide bandwidth of the system. Thus the received frequency f_{Rx} is always mixed by two frequencies offset from the transmit frequency by $\pm f_{LO}$. Consequently twice the image noise will enter the receiver and the number of unwanted mixer products is further increased.

4.1.3 Receiver using the Single VCO Transmitter

If a single higher frequency VCO is used in the transmitter (Subsection 3.1.2), the VCO output can be used directly in the receiver. The block diagram for a system in this configuration is shown in Figure 4-2.

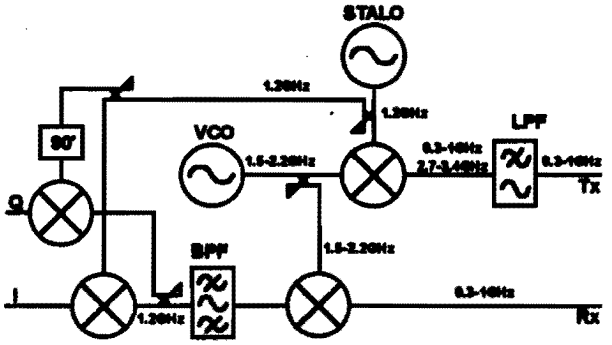

Figure 4-2: Receiver utilizing a higher IF

A stabilized oscillator is used in the transmitter to mix the higher VCO frequency range down to the required bandwidth of 300-1000 MHz. Only this lower side-band is transmitted, having passed through a low-pass filter in the transmit path. In the receiver, the VCO output can be mixed with the received signal to a high IF.

A major advantage of using a higher frequency VCO in this configuration is that the RF mixing signal is as spectrally pure as the VCO. It has not passed through any mixer and thus no unwanted mixer products are present in the signal driving the RF mixer. Furthermore, since only one frequency is driving the RF mixer at any time, the image-noise entering the receiver is minimized.

The signal can then be mixed down to a second lower IF stage for detection or detected at the high IF. Accurate I-Q detection at the frequencies above 1 GHz is difficult and thus a second lower IF stage is recommended. More importantly, a narrow band filter

is needed to minimize the system noise bandwidth and this is more easily realized at lower frequencies. Thus the system complexity is increased.

4.1.4 Two IF Stage up/down Receiver

A possible receiver design utilizing 2 IF stages by mixing first to a higher and then to a lower IF is shown in Figure 4-3. The design shown utilizes a 1.2 GHz first IF followed by a 10 MHz second IF stage.

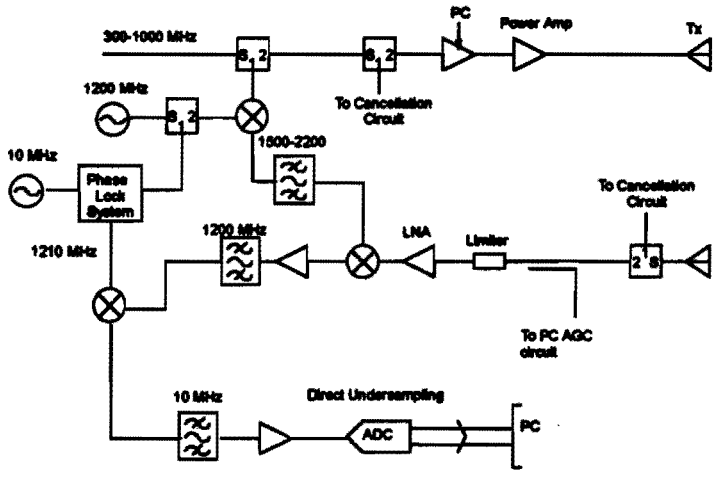

Figure 4-3: Receiver utilizing both a higher IF and a lower IF

A reference of the transmitted signal f_{Tx} is mixed with a higher first IF f_{IF1}. Choosing a high enough IF will make it possible to separate the sum and difference frequency bands of the first mixing signal. The required frequency separation depends on the filter used. Thus the received signal f_{Rx} is mixed only with the sum frequency $f_{Tx} + f_{IF1}$ resulting in improved image noise rejection and fewer unwanted mixer products. The difference frequency f_{IF1} is then bandpass filtered and mixed with $f_{IF1} + f_{IF2}$ to obtain a lower IF. This lower IF can then be I-Q detected.

This receiver combines the advantages of a high IF in terms of spurii rejection and those of a low IF in terms of noise bandwidth. However, the complexity is increased greatly and the two local oscillators must be locked together.

4.1.5 Frequency Synthesizer Receiver

If a frequency synthesizer is used in the transmitter, a second synthesizer locked onto the same reference can be used as the receiver. By tracking the transmit frequency at an offset, the receive synthesizer can be used to drive the IF mixer directly. Such a design was used by Iizuka et al [14].

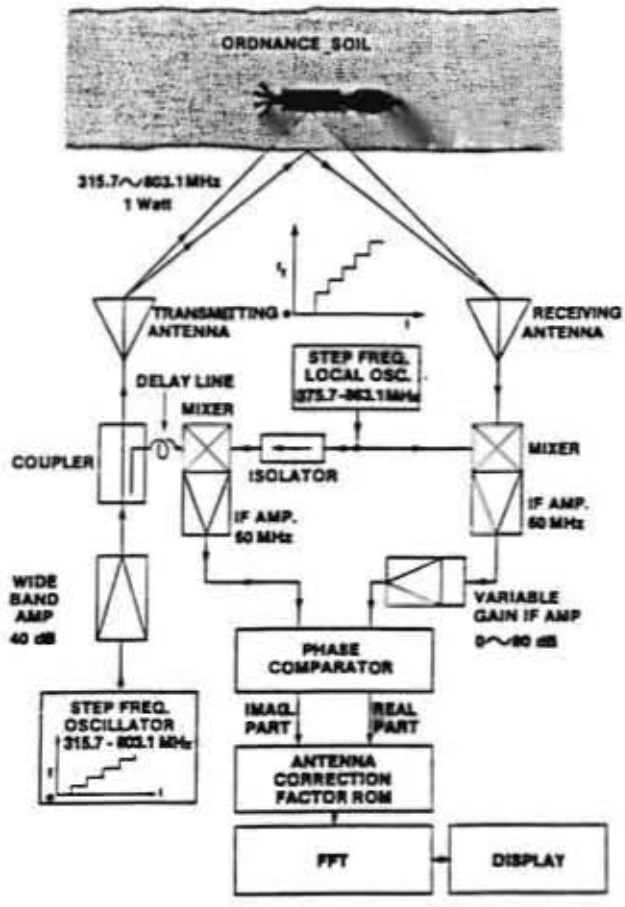

Figure 4-4: Block diagram of Radar used by Iizuka et al

The two frequency synthesizers used in the transmitter and the receiver can be seen to operate at offset frequencies. The receiver synthesizer steps through the frequency range 60 MHz above the transmit synthesizer. This signal is mixed with the received signal resulting in a 60 MHz IF. Mixing the signals from the two offset synthesizers results in a 60 MHz reference signal to which the received signal is compared.

There are numerous advantages to such a system: The frequencies can be made arbitrarily stable (at the expense of complexity) by using low reference frequencies. Thus a very narrow IF filter can be used resulting in excellent noise performance. Secondly,

the signal driving the IF mixer will be spectrally pure. As for the transmitter design (Subsection 3.1.4), the disadvantages in terms of complexity and expense put the frequency synthesizer out of the scope of the project.

4.2 I-Q Demodulation Designs

The full vector nature of the received signal has to be measured so that it can be resolved into the space domain by a complex FFT. Various designs that can be used to obtain the complex signal information are shown:

4.2.1 Conventional I-Q Detection

The conventional technique for measuring the in-phase and quadrature components of a signal is to split the signal into two channels. The first channel is mixed down with the IF frequency and the second channel is mixed with a 90° phase-shifted IF frequency. This can be seen in Figure 4-5.

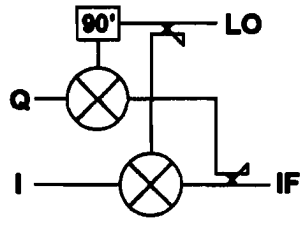

Figure 4-5: Conventional I-Q Detection using two mixers

The first advantages of such a system are that both I and Q are available simultaneously. Another advantage is that complete packaged I-Q detection systems are available with matched components [22].

Disadvantages include cross-coupling between the two channels, DC-offset and mixer matching. Cross-coupling is most evident when the phase is $\approx n\frac{\pi}{4}$ because there is a large difference between I and Q in these regions. The DC-offset due to the mixer imbalance varies with frequency and thus causes an error in both I and Q channels. The mixers as well as all the signal paths must be matched in phase so as to ensure minimum phase and amplitude imbalance.

4.2.2 Switched I-Q Detection

The switched I-Q detection method switches between in-phase and quadrature measurements by switching a $0°/90°$ phase shifter. This $0°/90°$ phase shifter can be located in either the transmitter or the receiver. However at RF frequencies the phase shifter must be accurate over the entire bandwidth, whereas the IF bandwidth is very much narrower. This makes it preferable to switch a $90°$ phase shifter in and out of the IF local oscillator path. An example of such a detection system using an IF phase shifter is shown in Figure 4-6.

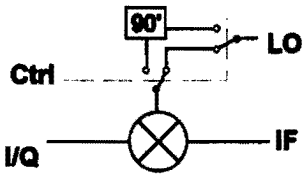

Figure 4-6: Switched I-Q Detection using a single mixers

The advantages of such a system include zero cross-coupling between the I and Q channels and the ability to measure dynamically the DC-offset of the mixer. There are also no imbalances between I and Q measurements.

4.2.3 Sub-Nyquist Quadrature Sampling

Since the IF bandwidth of a CW radar can be made arbitrarily narrow dependant only on the transmitter stability (Subsection 2.5.4), the signal can be sampled in quadrature at a sub-Nyquist rate [4], [8]. Quadrature sampling [8] can be used to reconstruct the signal by sampling the bandpass signal and its quarter wavelength translation at a common sampling rate dependant on an exact relationship between the center frequency and the bandwidth. Thus if the band is properly positioned, the IF can be sampled directly at a sampling rate of twice the bandwidth. This technique has been extended to a uniform sampling theorem [4].

The advantage of such a sampling system is that it is no longer necessary to mix the IF down to a lower frequency for sampling. The major disadvantage is that the transmitter and receiver have to be synchronized to a common reference. This system could thus be used in conjunction with a phase-locked loop transmitter. Other disadvantages include the need for a high speed sample-and-hold system.

4.3 RF Implementation

The single low IF double-sideband receiver design with conventional I-Q detection was chosen because the simplicity of the design made it possible to construct the receiver at a low cost and in a small space, thus making it possible to mount the receiver onto the back of the antenna. A double-sideband system had to be used because it was not the difficulty of constructing a single sideband modulator over a 700 MHz bandwidth made a single-sideband system very cumbersome.

Since a double-sideband system had been chosen, both the amplitude and phase of the received signal were modulated onto the amplitude of the IF with no information in the IF phase. Thus half of the unambiguous range could be extracted by detecting only the magnitude of the IF. This fact was overseen in the initial design stage and an I-Q demodulator was implemented. Since there is no information in the phase, an I-Q demodulator is redundant.

Although the advantage of mixing with a spectrally pure mixing signal in the single VCO receiver seemed to outweigh the advantages of other receivers, unwanted mixer products are transmitted by using this type of transmitter configuration (Subsection 3.1.2). These unwanted frequencies would then be received and thus degrade the receiver through interference. The two-stage- and the frequency synthesizer receiver designs were not used because of the high complexity and cost involved in such systems. The block diagram of the RF implementation showing the components used can be seen in Figure 4-7.

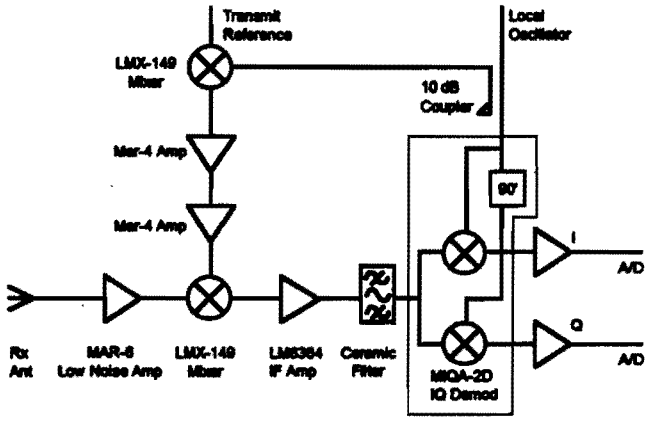

Figure 4-7: Receiver Block Diagram

For clarity, all mixer ports will be referred to as follows: the LO is the drive port, the RF is the high frequency (generally input) port and the IF is the low frequency (generally output) port. The received signal is amplified by a low-noise amplifier, applied to the RF port of the input mixer and then mixed down to a low IF. This IF is filtered and amplified, before being I-Q detected. The LO signal at the input mixer is generated by using the transmit reference to drive a mixer (LO port) with an IF input applied to the RF port. The transmit reference was used to drive the mixer because the harmonics of the LO are far greater than the harmonics of the RF. This resulted in a cleaner close-in frequency spectrum of the input mixing signal.

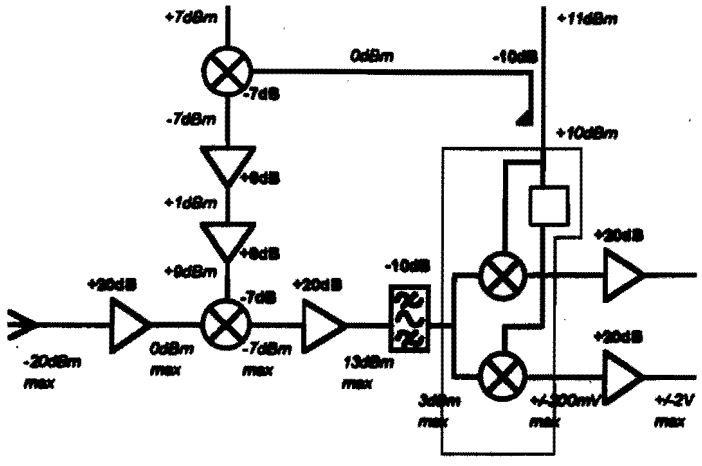

Figure 4-8: Receiver Power Budget - showing Gain, Loss (in bold print) and Maximum Power levels (in italics)

The power budget for the receiver is shown in Figure 4-8. The maximum power levels are derived from the 1 dB compression points of the components. A 0 dBm IF signal was mixed with a 7 dBm reference of the transmitted signal. This mixing signal was boosted through two amplifiers in order to drive the receiver mixer LO port. The maximum receiver input was calculated to be -20 dBm.

The receiver design was based on the specifications given by the manufacturers. After the components were chosen, they could not be tested individually, since their performance depended on the board layout of the final receiver design. Thus the board had to be designed and built based on component specifications, and only then could the individual components be tested. In this test phase it was discovered that the amplifiers operated below specifications and undocumented variations of mixer performance with frequency were found.

These problems caused the level of the mixing signal to be below the minimum required to drive the mixer sufficiently into saturation. Thus performance at high frequencies was degraded because the output of the mixer became dependant on the LO level towards 1 GHz.

4.3.1 Noise Performance

The system noise figure was calculated by the specifications and by measured parameters at 300 MHz and 1 GHz (Appendix A.2). The system noise figure and the dynamic range for these three cases are shown in Table 4.1.

	System Noise Figure	Dynamic Range
According to Specifications	3.31	76.7 dB
By measured 300 MHz values	3.69	76.2 dB
By measured 1 GHz values	7.34	73.3 dB

Table 4.1: System Noise Figure and Dynamic Range

The gain roll-off towards the upper frequency range doubles system noise figure at 1 GHz compared to 300 MHz. The dynamic range can be seen to decrease by 3 dB over the 300-1000 MHz frequency range. This dynamic range is further degraded by typically 20 dB due to feedthrough from the transmit into the receive antenna.

4.3.2 Low Noise RF Amplifier

The noise figure of the receiver is primarily dependant on the noise figure of the first stage [13]. However if the gain of the first stage is not sufficient, a high noise figure of the successive stage will increase the receiver noise figure significantly [24]. The noise figure for a system of N cascaded circuits is:

$$F_o = F_1 + \frac{F_2 - 1}{G_1} + \frac{F_3 - 1}{G_1 G_2} + ... + \frac{F_N - 1}{G_1 G_2 ... G_{N-1}} \tag{4.3}$$

The optimum first stage of a receiver is thus a low noise high gain amplifier. A suitable low cost amplifier to use in the RF front-end is the MAR-6 Mini-Circuits monolithic

amplifier [22]. The noise figure is 3 dB and the gain varies from 20 dB at 100 MHz to 16 dB at 1 GHz. Care has to be taken in the mounting of this amplifier to ensure proper operation. The PCB layout is shown in Figure 4-9. This has been adapted from the design recommended by the manufacturer [22, 3-11].

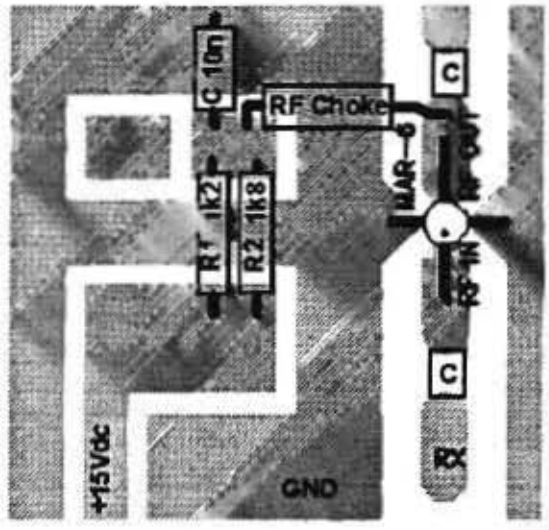

Figure 4-9: Front-end Low Noise RF Amplifier using the MAR-6

The required bias voltage and current at the output of the MAR-6 are 3.5 V and 16 mA respectively. The required bias resistance can thus be found using the following formula [22, 3-10].

$$R_{bias} = \frac{V_{CC} - V_{bias}}{I_{bias}} = 719\Omega \tag{4.4}$$

for a supply voltage of 15 Vdc. $R_{bias} = 720\Omega$ is realized by R1 ($1.2k\Omega$) and R2 ($1.8k\Omega$) in parallel. The supply is fed to the output of the MAR-6 amplifier on the microstrip line with a series RF choke. The choke is realized by 5 turns of wire on a ferrite bead and serves the dual purpose of isolating the line impedance from the bias resistance and preventing RF leakage into the power supply. Furthermore, a $10\mu F$ bypass capacitor was used to provide a short circuit path to ground for any RF leakage that should manage to get through the choke.

The two blocking capacitors in the microstrip line serve to isolate the amplifier in DC from the rest of the circuit. The choice of capacitors was found to be critical in the performance of the amplifier. The low frequency limit is due to the impedance of the capacitor at 300 MHz. The impedance should be small compared to 50Ω, the characteristic impedance, so as to provide an RF short ($Z_{300MHz} = \frac{1}{2\pi fC}$). The high frequency

limit is due to the resonant frequency of the capacitor due to parasitic inductance. By setting the resonant frequency to above 1 GHz, a value for the maximum parasitic inductance can be found ($L_{max} = \frac{1}{4\pi^2 f^2 C}$ where f = 1 GHz). Table 4.2 shows impedance, standing-wave ratio and maximum internal inductance values for various capacitances:

C	Z [Ω]	VSWR	Z [Ω]	VSWR	L_{max}
	300 MHz		1GHz		
10 pF	53.1	2.1	15.92	1.32	2.53 nH
100 pF	5.31	1.11	1.59	1.03	253 pH
200 pF	2.65	1.05	0.78	1.02	127 pH
500 pF	1.06	1.06	0.32	1.006	50.7 pH
1 nF	0.53	1.01	0.16	1.003	25.3 pH

Table 4.2: Capacitive Impedance, Voltage Standing-Wave Ratio and Maximum permissible Internal Inductance for various Blocking Capacitor Values

The VSWR is the input voltage standing wave ratio of the capacitor in series with the 50Ω line. The maximum input VSWR of the MAR-6 amplifier is quoted as 1.5:1 by the manufacturer, and thus the VSWR of the capacitor should be less than this so as not to degrade the input match of the amplifier. Thus the capacitance cannot be less than 100 pF. Typical values for parasitic inductance in chip capacitors vary from 1-0.1 nH. Choosing either a 100 pF or 200 pF capacitor would thus balance out these two effects.

Since the amplifier is a part of the larger receiver board, it was tested by disconnecting the outer edges of the RF blocking capacitors. Coaxial cables were soldered onto the edges and the system was tested with a network analyzer. Testing the amplifier in this way was not optimal because the cables and the connections introduced unwanted frequency responses. However, testing the amplifier in a separate rig would not include the effect that the specific board layout has on the circuit. The frequency response for the MAR-6 amplifier measured in this way is shown in Figures 4-10 and 4-11.

The manufacturer quoted the gain to vary from 20.1 dB at 100 MHz, and 18.7 dB at 500 MHz to 16.4 dB at 1 GHz. The magnitude of the measured frequency response can be seen to vary considerably from the quoted gain for the amplifier (16.2 dB at 500 MHz and 12.2 dB at 1 GHz). At least a 1dB loss can be expected from the crude measurement method, with an increasing loss with frequency. Other sources of reduced gain are the effect of the blocking capacitors and the board layout.

The effect of this large gain variation with frequency on the noise figure can be seen by looking at 300 MHz and 1 GHz. At 300 MHz, the noise figure at the output of the

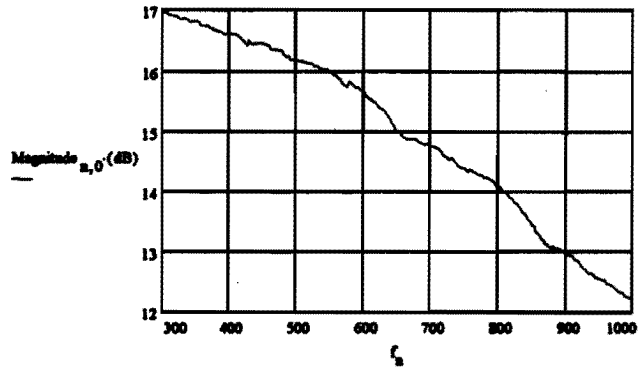

Figure 4-10: Magnitude Response of the MAR-6 Low Noise RF Amplifier

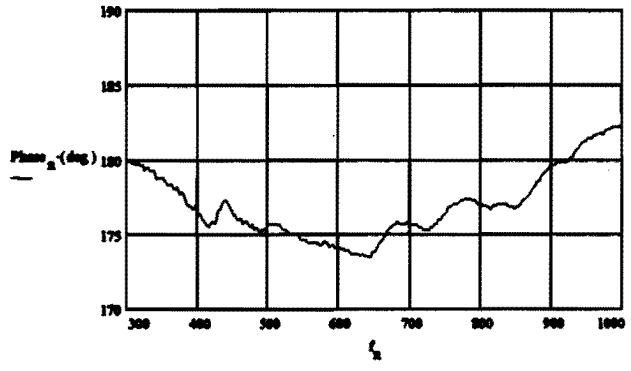

Figure 4-11: Phase Response of the MAR-6 Low Noise RF Amplifier

mixer will be:

$$NF_{300MHz} = NF_{MAR6} + \frac{NF_{Mixer} - 1}{G_{MAR6@300MHz}} = 1.91 + \frac{4.37 - 1}{50.1} = 2.95dB \qquad (4.5)$$

where $NF_{MAR6} = 2.8dB = 1.905$, $NF_{Mixer} = 6.4dB = 4.365$ and $G_{MAR6@300MHz} = 17dB = 50.1$. At 1 GHz, the gain was decreased significantly and the mixer loss has increased, resulting in a greater mixer noise figure.

$$NF_{1GHz} = NF_{MAR6} + \frac{NF_{Mixer} - 1}{G_{MAR6@1GHz}} = 1.91 + \frac{6.40 - 1}{16.6} = 3.28dB \qquad (4.6)$$

where $NF_{MAR6} = 2.8dB = 1.905$, $NF_{Mixer} = 8.1dB = 6.40$ and $G_{MAR6@1GHz} = 12.2dB = 16.6$. Thus the noise figure can be seen to increase by 0.33 dB at 1 GHz because of the gain variation. In addition, the dynamic range at 1 GHz is decreased by 4.8 dB because of this gain variation. In addition, the system noise figure will be decreased because of this reduced gain (Table 4.1).

4.3.3 Mixers

The mixing system consisted of two mixers and two monolithic amplifiers. A fraction of the transmit signal was mixed with the IF frequency. This signal is amplified so as to be used to drive the receiver mixer. LMX-149 Mini-Circuits mixers were used for both the reference mixer and the receive mixer. The frequency range was 10-1500 MHz for the LO/RF ports and DC-1500 MHz for the IF port. This mixer was chosen because mixer performance starts to degrade towards the upper frequency range (conversion loss increases, isolation decreases). Thus the area of operation (10-1010 MHz) was mostly in the mid-band. The conversion loss of the mixer was specified to have a mean of 6.6 dB.

The reference mixer was driven by a 10 dBm reference signal on the LO port. A 0 dBm 10.7 MHz signal was input on the RF port and the IF output which included the sum and difference frequencies was connected to the driving amplifier chain.

The receiver mixer was driven by the two sidebands which had been amplified by the driving amplifier chain. The RF port was connected to the output of the MAR-6

low-noise front-end amplifier. The IF port was connected to the 10.7 MHz IF amplifier.

The complete mixing system board layout showing the reference mixer, the driving amplifier chain and the receive mixer is shown in Figure 4-12.

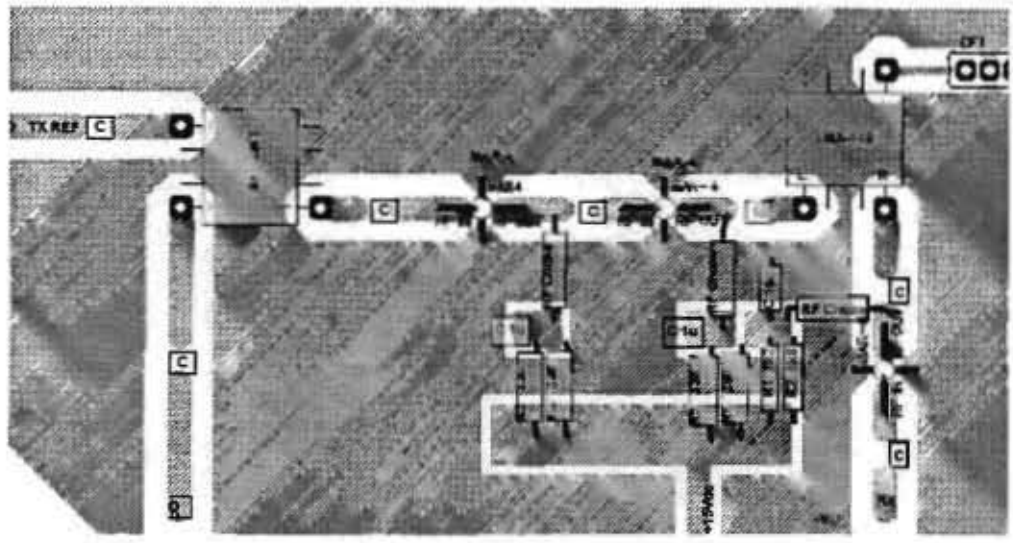

coupled
through surface mount blocking capacitors. The output is connected to the MAR-4 amplifier chain. The amplifiers are separated by blocking capacitors. The output of the amplifier chain is connected to the LO port of the receive mixer. The output of the receive mixer is connected the IF circuit.

4.3.4 Driving Amplifier Chain

The output of the reference mixer had to be amplified to the range 4-10 dBm so as to drive the receive mixer into saturation. Two cascaded Mini-Circuits MAR-4 monolythic amplifiers were used for this purpose. These amplifiers have a quoted gain of 8.3 dB at 100 MHz decreasing to a gain of 8 dB at 1 GHz. The cascade can be seen as part of the mixing system in Figure 4-12. The required bias voltage and current at the output of the MAR-4 amplifiers are 5.25 V and 50 mA respectively. The required bias resistance for each amplifier can thus be found using the following formula [22, 3-10].

$$R_{bias} = \frac{V_{CC} - V_{bias}}{I_{bias}} = 180\Omega \tag{4.7}$$

for a supply voltage of 15 Vdc. $R_{bias} = 180\Omega$ for the first MAR-4 is realized by R3 (330Ω) and R4 (390Ω) in parallel. A parallel resistor configuration was used to reduce the power dissipation to less than 200 mW per resistor. Thus 1/4 W resistors could be used for the bias network. The supply is fed to the output of the MAR-4 amplifier on the microstrip line with a series RF choke. The choke is realized by 5 turns of wire on a ferrite bead and serves the dual purpose of isolating the line impedance from the bias resistance and preventing RF leakage into the power supply. A 10μ F bypass capacitor was used to provide a short circuit path to ground for any RF leakage that should manage to get through the choke. The measured frequency response for the 2 MAR-4 amplifiers in cascade is shown in Figures 4-13 and 4-14.

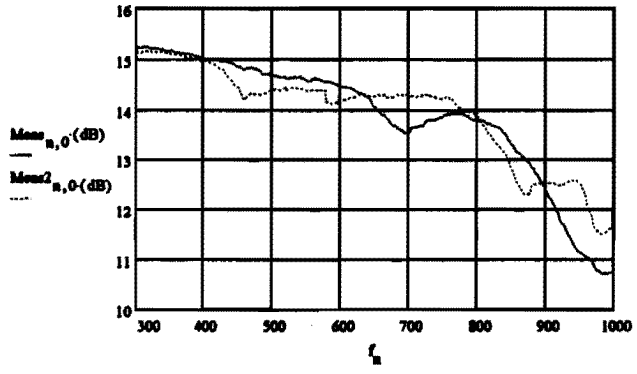

Figure 4-13: Magnitude Response of the MAR-4 Amplifier Cascade

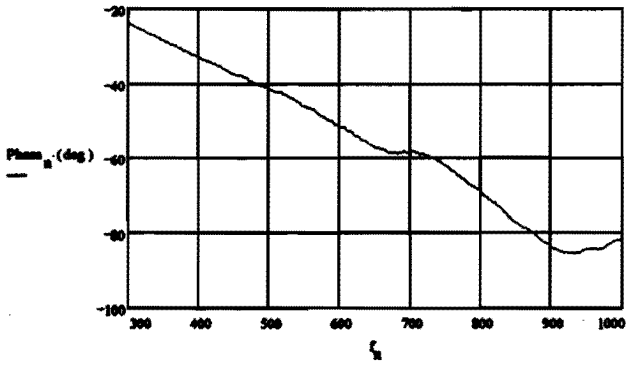

Figure 4-14: Phase Response of the MAR-4 Amplifier Cascade

The manufacturer quoted the gain to vary from 16.6 dB at 100 MHz, and 16.4 dB at 500 MHz to 16 dB at 1 GHz for the two MAR-4 amplifiers in cascade. The magnitude of the measured frequency response can be seen to vary considerably from the quoted gain for the amplifiers (14.7 dB at 500 MHz and 10.8 dB at 1 GHz). The effect of the

crude measurements technique can be seen in the two curves of Figure 4-13 which are two measurements of the gain with variations caused by moving the connection cables.

4.4 IF Implementation

The reasons for the choice of I-Q demodulator, given the earlier oversight, are: A conventional I-Q demodulator was chosen because of the availability of a packaged Mini-Circuits I-Q demodulator. The advantages of a switched I-Q demodulator, namely zero I-Q coupling and the ability to measure dynamically the DC-offset, were not significant for the double-sideband receiver implementation. This is because the I and Q channels are always 180° out of phase. There is thus no added information in the Q channel. The DC-offset is not a problem because the IF amplitude varies sinusoidally. A sub-Nyquist sampling system could not be used because of the RF design chosen.

4.4.1 IF Oscillator

A Colpitts crystal oscillator was used to generate the 10.7 MHz IF signal. The schematic for the oscillator can be seen in Figure 4-15.

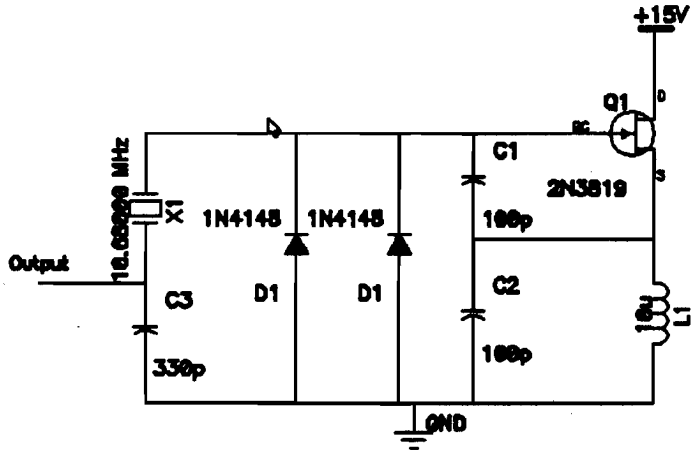

Figure 4-15: 10.68 MHz Local Oscillator

The output of the oscillator has bandpass filtered with a 10.7 MHz ceramic filter and distributed to provide 0 dBm at the reference mixer RF input and 10 dBm at the I-Q demodulator LO input. The harmonics levels were kept below 60 dBc.

4.4.2 IF Filter

A 10.7 MHz ceramic filter was used as the IF filter. This filter was chosen because of easy availability and relatively high Q. The bandwidth of this filter was measured to be 200 kHz and the insertion loss 10 dB. The bandwidth was sufficient to cover the 40 kHz frequency-jitter observed in the transmitter (Subsection 3.3.3). Thus if the difference between the transmit frequency and the received frequency is greater than 200 kHz, the signal will be degraded by the IF filter. The frequency response of the IF filter is shown in Figure 4-16.

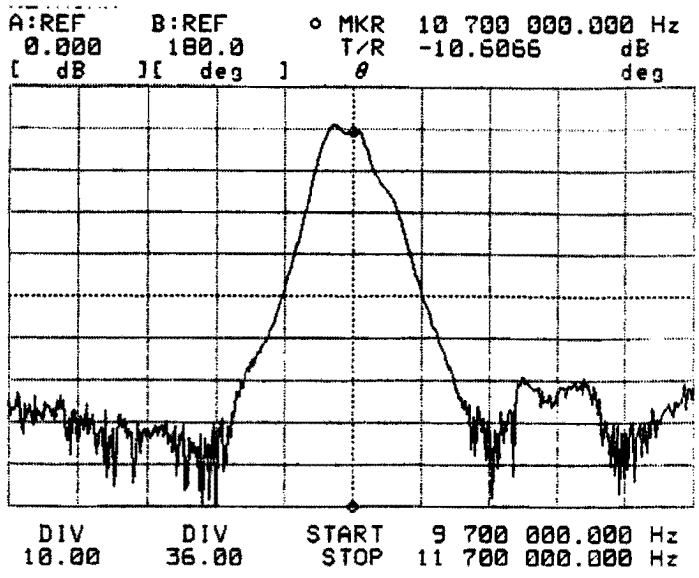

Figure 4-16: Frequency Response of the IF Ceramic Filter

A narrower IF filter would reduce the IF noise floor and thus prevent IF saturation on noise. It can be seen that a high error margin was given to the frequency jitter and this could be reduced. However, the chance of signal degradation would then be increased. Thus only improvements in CW transmitter stability would warrant a reduction in IF bandwidth.

4.4.3 IF Amplifier

An LM 6364 operational amplifier (opamp) with a fixed voltage gain of 10 was used as an IF amplifier. This opamp was chosen for its high gain-bandwidth product of 175 MHz. The opamp is stable for gains greater than +5. This voltage gain corresponded to a +20 dB power gain and would have been sufficient had the RF components performed to specification. Because of the lower gain in the MAR-6 LNA and the

greater losses in the mixer, the gain was not sufficient to optimize the dynamic range. The voltage gain was subsequently increased to 15 (23.5 dB), whereby the output level of the IF amplifier with a -20dBm receiver input was measured to be -5 dBm. This was still well below the 1-dB compression point of the I-Q demodulator at +4dBm.

A solution to the problem of quantization error of small signals due to the A/D, would be to add a variable-gain IF amplifier to the fixed gain amplifier.

4.4.4 IF I-Q Demodulation

A Mini-Circuits MIQA-10D I-Q demodulator was used to detect the in-phase and quadrature components of the IF signal. This I-Q demodulator was not strictly necessary, since a double-sideband system was implemented. Thus both the amplitude and phase of the received signal were modulated onto the amplitude of the IF with no information in the IF phase. A 10 dBm 10.7 MHz signal was applied to the LO port and the output of the IF amplifier was matched to the RF input. A 50Ω external termination was realised with 2 100Ω resistors in parallel. Since both I and Q varied sinusoidally with frequency, the DC offset was easily calibrated out by shifting the zero point. The maximum voltage swing that could be obtained by the demodulator was ±200 mV.

4.4.5 DC Amplifier and A/D Conversion

The DC voltage outputs for the I and Q channels of the I-Q demodulator were measured to be within the range ≈ -200 mV to 200 mV. These voltages were then amplified by instrumentation amplifiers with a gain of 10 and sampled with 12-bit analogue-to-digital converters covering the range -2.5 V to 2.5 V. A PC-74 card in a 386 PC was used to do both the amplification and the A/D conversion. The data values were then be stored in memory and saved to disk at the end of a scan.

The software programmable instrumentation amplifiers on the PC-74 card could be programmed for gains of 1, 10, 100 or 500. Using the instrumentation amplifiers with a fixed gain of 10 had the disadvantage of wasting 10% of the available A/D range for both positive and negative voltages. A separate amplifier with a gain of 12.5 would increase the dynamic range accordingly.

A photograph of the complete receiver board in the testing phase is shown in Figure 4-17. Note the coaxial cables soldered directly onto the PCB.

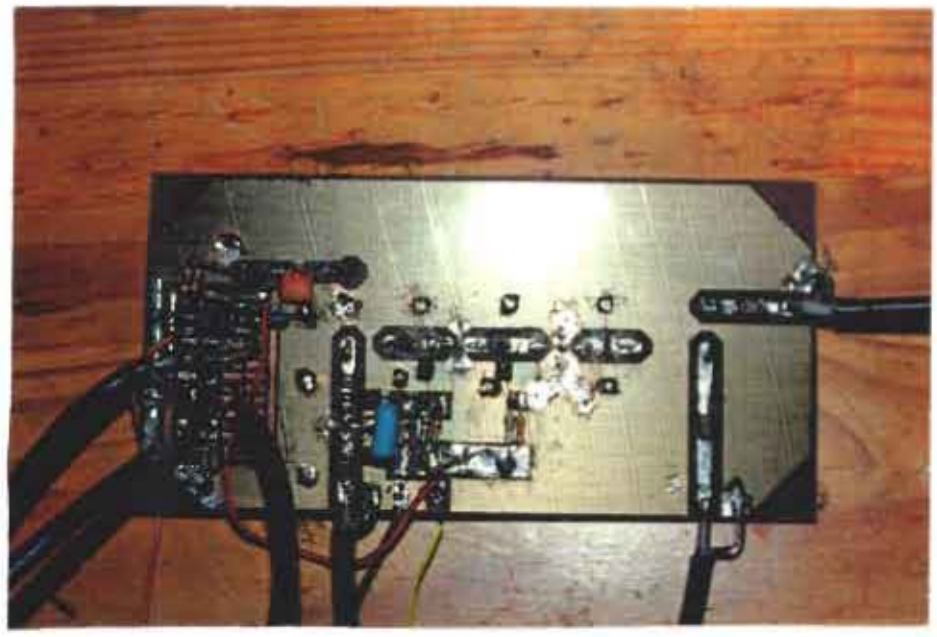

Figure 4-17: Photograph of the Prototype Receiver Board in the Testing Phase

4.5 Receiver Performance

4.5.1 Spectral Purity of the Mixing Signal

An IF of 0 dBm was applied to the RF input port of the mixer in order to generate as large as possible a mixing signal. However, due to two-tone third order distortion, unwanted products up to -30 dBc were observed. This can be seen in the plot of the frequency spectrum shown in Figure 4-18.

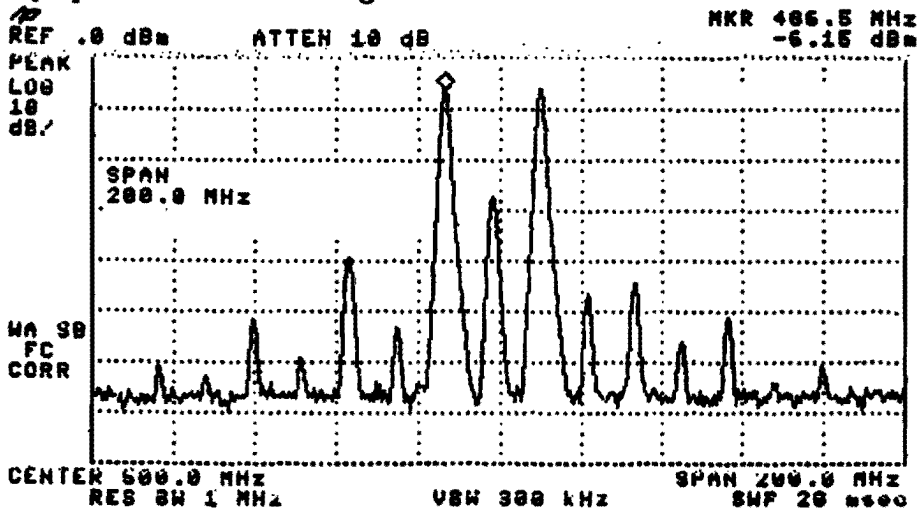

Figure 4-18: Frequency Spectrum of Mixing Signal for a 0dBm IF input

The frequency spectrum can be seen to be extremely cluttered. Since the received signal is mixed by all these frequencies, some unwanted products will fall onto the IF band causing errors. Reducing the IF signal level to -10 dBm resulted in a reduction of unwanted products to -50 dBc. This is shown in Figure 4-19.

The frequency spectrum of the mixing signal is seen to be less cluttered. However since the sideband signal level has been decreased, the gain in the driving amplifier chain would have to be increased by 10 dB. Reducing the IF signal level to -70 dBm resulted in a reduction of unwanted products below -70 dBc. This would thus provide an optimally clean frequency spectrum for a mixing signal, but another problem in the reference signal feedthrough was observed.

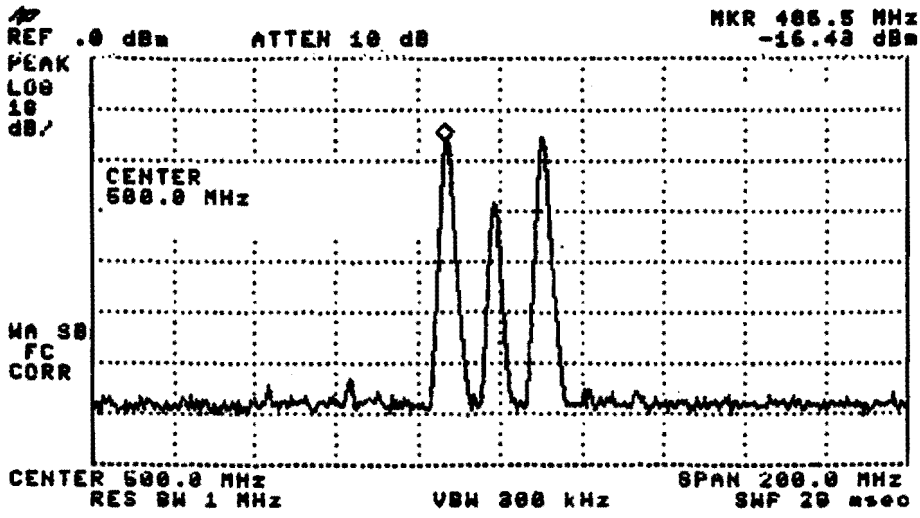

Figure 4-19: Frequency Spectrum of Mixing Signal for a -10dBm IF input

4.5.2 Reference Signal Feedthrough into the Mixing Signal

The LO-IF isolation of the mixer was found to vary by up to 20 dB over the frequency range. This can be seen in Figure 4-20.

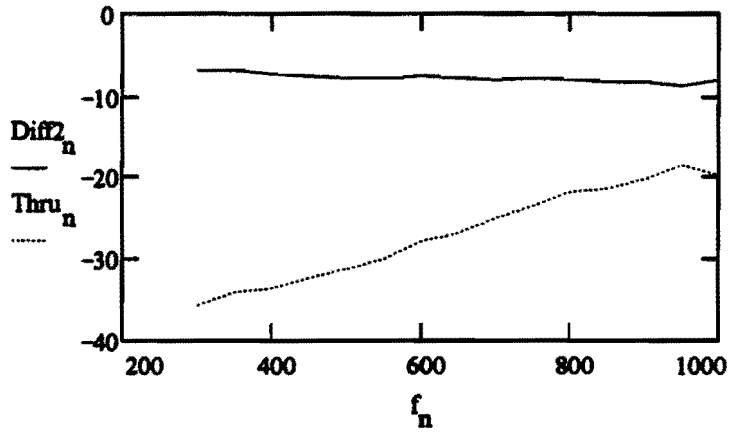

Figure 4-20: Plot of Sideband and LO-IF Feedthrough for IF=0dBm

At 300 MHz the LO-IF isolation can be seen to be 46 dB, decreasing to 29 dB at 1 GHz. This was not a problem for the design as it was implemented, since the level of the sidebands can be seen to be at least 10 dB above the feedthrough. However, since the LO-IF feedthrough depends only on the LO level, a -10 dBm IF input will be of the same level as the LO feedthrough at 950 MHz. This can be seen in Figure 4-21.

At 950 MHz, the LO-RF feedthrough signal can be seen to be 2 dB greater than the sidebands. Figure 4-22 shows the frequency spectrum of the mixing signal for a 950 MHz LO reference signal. This feedthrough signal will leak through into the

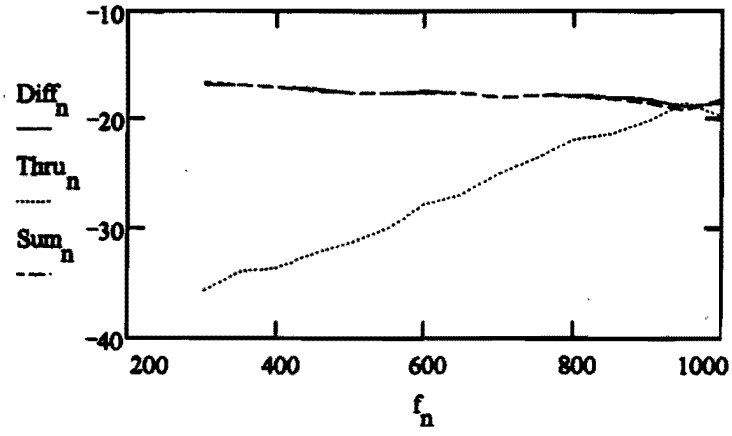

Figure 4-21: Plot of Sideband and LO-IF Feedthrough for IF=-10dBm

RF input and appear as a target. The level of this feedthrough target will be the approximately -40 dBm.

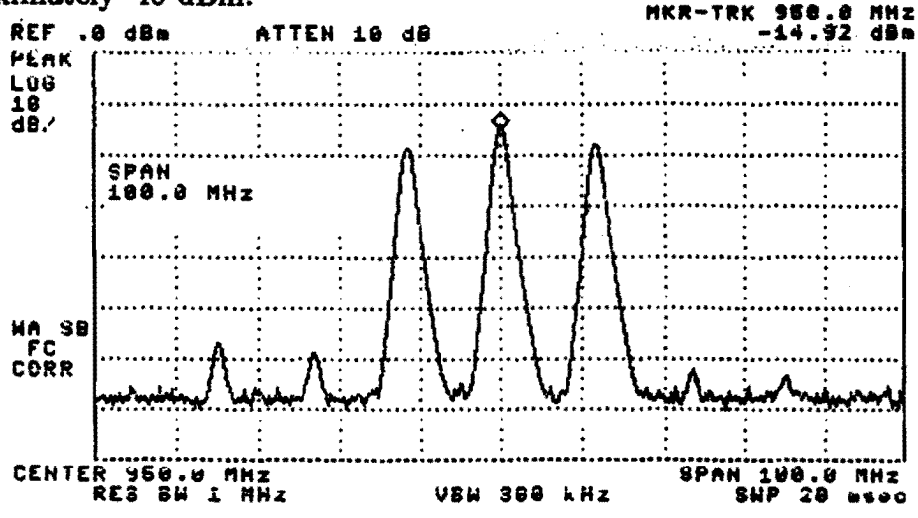

Figure 4-22: Frequency Spectrum of Mixing Signal for a -10dBm IF input at 950 MHz

If the IF input to the mixer is decreased to -20 dBm, the feedthrough signal would be 10 dB greater than the sidebands at 950 MHz. This is clearly unacceptable, because the feedthrough will saturate the driving amplifiers and could also damage the receiver mixer. Thus the optimal trade-off between unwanted products and reference feedthrough is an IF level of approximately -10 dBm. This does however raise the level of the feedthrough signal by 10 dB compared to the IF = 0 dBm case.

4.5.3 Receiver Dynamic Range

The receiver dynamic range was measured by varying the input signal strength and observing the location of the 1 dB gain compression point. From this point, the signal was decreased until the signal was observed to be 10 dB above the noise floor. In this manner, a 50 dB dynamic range was observed. This is significantly less than the calculated dynamic range.

The dynamic range was reduced by the less than optimal IF and DC gain stages. The dynamic range can be improved optimizing the IF gain stage and the DC gain stage. A variable gain 10.7 MHz amplifier with a gain of 20-40 dB and a DC amplifier with a voltage gain of 12.5 would increase the dynamic range by at least 20 dB.

Chapter 5

Feedthrough Cancellation

Direct coupling between the transmit and receive antennas of continuous wave radars limits the dynamic range of the receiver by inserting a large unwanted signal into the receiver front-end. This coupling signal is typically 20 dB above the strongest target reflection.

Pulsed radar systems overcome this direct coupling problem by time-domain gating the receiver. Since the wanted signal is of the same frequency as the coupling, filters as in doppler radars cannot be used. Thus the only solution is to add some vector to the received signal which will cancel the large coupling feedthrough. Various techniques exist to cancel some of the coupling over narrow bandwidths, but modern components can extend these techniques to allow cancellation over octave or greater bandwidths. Some of the techniques that will be discussed involve digital control of coupling reduction, cancellation at IF and RF sections and feedback techniques to take into account ageing of the antenna and other components.

5.1 A Summary of Feedthrough Cancellation Techniques for CW Radar

Continuous wave radar works on the principle that the phase shift of the returned wave is proportional to the distance to the target. Thus a target situated at a distance of R will cause a phase shift of

$$\phi = \frac{4\pi R}{\lambda} \tag{5.1}$$

at the receive antenna. Since only variations of 2π can be detected, such a system would have an unambiguous range limited to half the wavelength of the transmit frequency. Thus some modulation scheme has to be used to increase the range of the radar. The two modulation techniques most widely used are frequency modulation (FMCW) and frequency stepping (SFCW).

Since continuous waves are used in CW radar, the transmitter and receiver have to both be on at all times. In comparison, a pulsed radar system can switch the receiver off during the transmission period. Having both transmitter and receiver on at all times can bring on the following problems due to feedthrough from transmitter to receiver:

- Decrease in Receiver sensitivity
- Saturation of Receiver
- Destruction of Receiver

These are listed in increasing order of severity. A small amount of feedthrough will only decrease the sensitivity and thus the dynamic range of the receiver. If enough power is fed into the front end amplifier of the receiver to exceed the 1 dB saturation point, the received signal will be distorted and unusable. Should the feedthrough exceed the maximum [no damage] input power of the receiver, the receiver will be damaged.

In order to reduce the feedthrough, most CW radar systems use separate transmit and receive antennas to achieve some isolation [24, p71-p74]. In most applications, this is insufficient.

Passive feedthrough cancellation techniques can be used in CW doppler radars: in effect a narrow band band-pass filter at the transmit frequency. Such a filter would not be feasible for SFCW or FMCW schemes and thus an active feedthrough nulling technique is needed.

5.1.1 Cancellation Systems

A cancellation system needs to control the amplitude and phase of the cancellation signal in order to obtain a signal that is equal in amplitude and 180° out of phase relative

to the feedthrough signal. Thus the properties of the feedthrough signal must be well known and repeatable. If a single frequency, represented by $E_o e^{-jwt}$, is transmitted, the received signal can be approximated by a sum of point targets [15]. The feedthrough signal can thus be shown as a target at a distance equal to the feedthrough path.

In a lossless homogeneous medium with n point-type scatterers, the return including the feedthrough signal will be:

$$Rx\alpha\frac{E_o}{d_f^2}s_f e^{j(2\beta_f d_f - wt)} + \sum_{i=1}^{n}\frac{E_o}{d_i^2}s_i e^{j(2\beta d_i - wt)} \tag{5.2}$$

where E_o = field strength of emitted signal
d_i = distance to i^{th} target
d_f = equivalent feedthrough path
s_i = radar cross section of the i^{th} target
s_f = equivalent feedthrough strength
β = propagation constant for the media
ω = transmit frequency

Thus the received signal will be a vector sum of all the scatterers and the feedthrough signal. To cancel the feedthrough signal, an appropriate vector has to be generated and added to the received signal. A vector representation of the signals involved is shown in Figure 5-1.

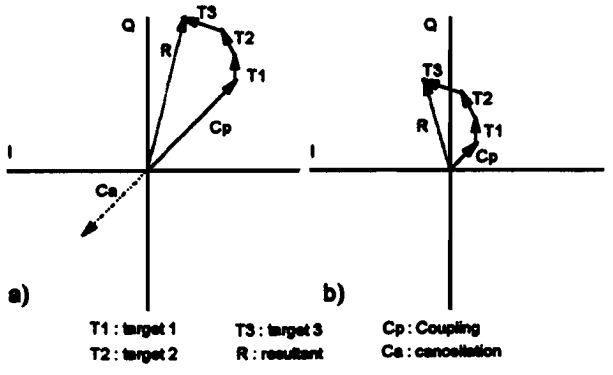

Figure 5-1: Vector map of signals in a SFCW radar system. The first plot shows the composition of the received signal and the second plot shows the effect of the cancellation signal

The effect of an amplitude or phase imbalance in the coupling signal is that the amount

of feedthrough will increase proportional to the imbalance. A phase imbalance is more critical. It can cause false targets to appear. In closed loop systems, a phase imbalance can cause the system to go unstable. Thus a vector has to be created to track the feedthrough signal over the complete system bandwidth with a 180° phase shift. This is relatively simple to do over narrow bandwidths, but becomes very difficult at wider bandwidths. Ageing of the system leads to a change in the feedthrough characteristic and this will cause imbalances in phase and amplitude.

Transmission Line Cancellation

The most basic type of cancellation circuit can be constructed using a length of transmission line to achieve an 180° phase shift with a programmable attenuator to adjust the amplitude of the cancellation signal. The electrical length of the transmission line must differ from the feedthrough path by 180°. The bandwidth of such a system is only about 10% of the center frequency. It would be possible, however, to have a bank of different length lines and to switch them according to the transmit frequency. The block diagram for such a system is shown in Figure 5-2.

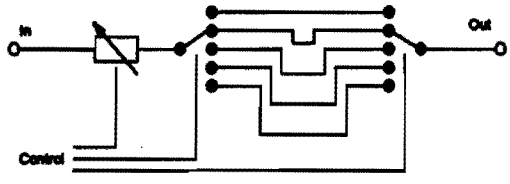

Figure 5-2: Transmission Line Cancellation Circuit with a single attenuator and different lengths of line

Such a system has the advantage of being extremely robust. The maximum power that can be handled by such a system depends only on the attenuator. However, it is impossible to calibrate the phase once the lengths of transmission line have been set, making this system impractical for most applications. The physical size of the system is another disadvantage, especially if a large number of transmission lines are needed to cover the bandwidth.

Magnitude-Phase Cancellation

A magnitude-phase cancellation system consists of a programmable attenuator in series with a programmable phase shifter. Either an 180° phase shifter with an analogue modulator or a 360° with a programmable attenuator can be used. The control signals have to be received in, or converted into, magnitude-phase representation to control the cancellation circuit. The following Figure 5-3 shows two different configurations:

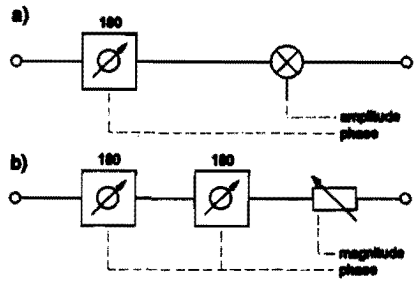

Figure 5-3: Magnitude-Phase Cancellation Circuits a) 180° phase shifter with analogue modulator b) 360° phase shifter with attenuator

Phase shifters are only available for maximum bandwidths of 30% of centre frequency, which limits this system to narrow bandwidth applications. Due to the large phase shifter control voltage transient when the phase flips at 360° degrees, this system is not suitable for FMCW [2]. This is because FMCW is modulated in time. For SFCW systems, this does not pose a problem, since a wait time can be inserted at the phase change. Another point is that the phase response of the attenuator and the magnitude response of the phase shifter have to be taken into account in the control voltages.

I-Q Cancellation

Voltage controlled phase shifting devices are available only over narrow bandwidths and seldom over a whole 360° phase shift. Although it would be possible to cascade phase shifters, a more common approach is to control the magnitude of both the in-phase (I) and quadrature (Q) components of the cancellation signal simultaneously. This method gets rid of phase control altogether. However, the 90° phase shift has to be accurate over the whole bandwidth in order to avoid cross-coupling between the two control paths, which can lead to instability in a closed loop cancellation system. The cancellation system has to controlled in all four quadrants and thus both I and Q channels have to modulate in amplitude and in sign. Two methods of achieving such I-Q modulation are shown in Figure 5-4.

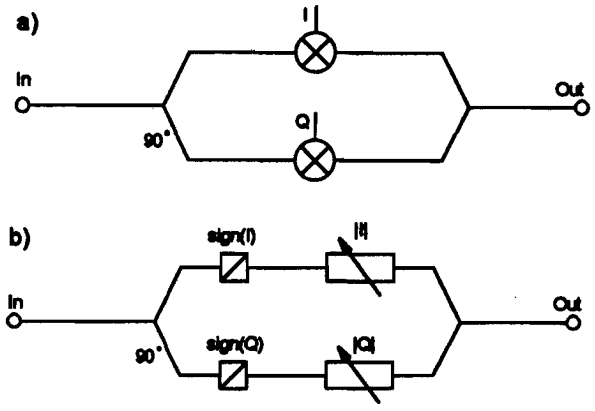

Figure 5-4: I and Q Cancellation Circuits a) analogue biphase modulator b) sign and amplitude control

Such a system can be constructed for wide bandwidths, with the limiting component being the 90° power splitter. These have recently become available in multi-octave bandwidths [21]. Thus good orthogonality can be ensured over multi-octave bandwidths. It is also more practical to receive the signal in I-Q than extracting magnitude and phase information accurately.

5.1.2 Reduction Control

There are basically two methods of controlling the feedthrough cancellation circuit. The first method would be to measure the coupling and use the stored values as control parameters. The second method would be to close the loop and thus have an adaptive cancellation circuit.

Stored value control

If the feedthrough signal is well behaved in time, the coupling signal can be measured once over the entire system bandwidth and then stored in memory. Then, at each transmit frequency, the appropriate parameters can be called up and used to control the cancellation circuit. Any slow variations with time can be dealt with by calibrating the system at regular intervals. However, any large changes in the feedthrough signal between calibrations will cause large errors in the received signal. Since a memory of the coupling vector is required, digital implementation and control is necessary, which

can be seen in Figure 5-5 .

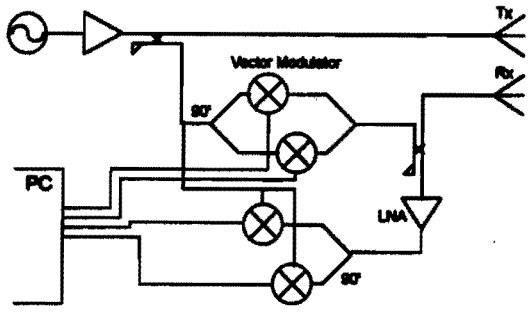

Figure 5-5: Stored Value Control using a computer as memory and control device

A problem is that calibration can be difficult. A possible solution would be to have a suitable attenuator that can be switched into the receiver path, so that the coupling can be measured without saturating the receiver. Since this is only for calibration, a decrease in sensitivity is not a problem. The received signal would have to be processed to resolve the coupling vectors from targets at other ranges. These values can then be stored as control values.

Closed Loop Control

If the coupling vector can easily be distinguished within the received signal, a closed loop control system can be implemented. This constraint shows that closed loop control is possible for FMCW systems, but not easily implemented in SFCW systems where DFT processing is required to resolve the coupling vector. In a closed loop control system, the received signal must be resolved into its vector components. These control the cancellation signal through a vector modulator. Care must be taken to prevent cross-coupling between the two feedback paths. According to Harmer [9], the phase has to be aligned within 10 or 20° for stability to be maintained. A cancellation system utilizing closed loop control is shown in Figue 5-6.

A closed loop I/Q cancellation X-band system has been successfully implemented into the 'PILOT' FMCW radar [2]. This system showed 33-40 dB of cancellation over bandwidths of 400-1000 MHz at X-band, depending on the antenna tested. A problem with closed loop control is that amplitude modulators do not attenuate linearly with control voltage. Thus a linearizing circuit is necessary.

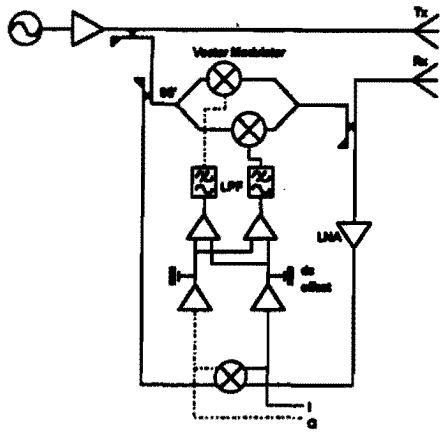

Figure 5-6: Closed Loop Control

5.1.3 Position of Cancellation System

The positioning of the cancellation circuit depends on the severity of the feedthrough. If the feedthrough is so large that it will saturate the IF section, the cancellation system has to be implemented in RF. If the dynamic range of the IF system is sufficient, however, the cancellation can be implemented inside the IF stage. Closed loop control can be implemented in either positions.

RF Cancellation

An RF cancellation system is positioned immediately before the first mixer stage into the IF system. The level of feedthrough signal that can be nulled in this way is thus limited only by the RF amplifiers. Figure 5-7 shows an RF cancellation system.

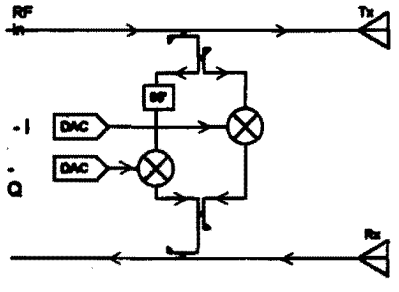

Figure 5-7: Cancellation in the RF section

The disadvantage of this positioning is that the cancellation circuit has to operate over the complete sweep bandwidth. RF cancellation systems using ferrite microwave

and varactor modulators are descibed by Harmer [9]. However, advances in microwave components have made it possible to use conventional techniques at higher frequencies.

IF Cancellation

The cancellation can be done in the IF stage if the dynamic range of the RF assembly is sufficient for both feedthrough and signal. A cancellation system utilizing this positioning is shown in Figure 5-8.

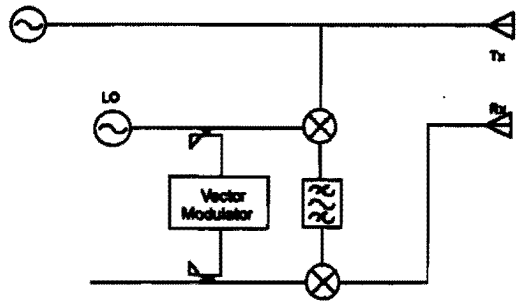

Figure 5-8: Cancellation in the IF section

The advantage of this positioning is that the feedthrough vector needs to be controlled at a single frequency only. This is achieved by mixing the received RF signal with a frequency shifted version of the transmit signal. Thus a single frequency IF in achieved and the cancellation circuit can be operated at a single frequency, independant of sweep bandwidth.

The level of feedthrough has to be low enough, so as not to saturate the RF amplifiers nor the IF mixer stage. This position lends itself to wide band systems, since the bandwidth is not dependant on the cancellation circuit. The bandwidth of operation of feedthrough cancellation systems depends on how accurately the feedthrough signal can be tracked in magnitude and phase. Some of the above systems lend themselves more readily to wide band systems. Advances in 90° power splitter design have extended the operational ability of I-Q cancellation systems into multi-octaves. Wide band amplifiers are becoming available with improved gain flatness. Through component advances, feedthrough nulling techniques are becoming more accurate and possible over wider bandwidths.

5.2 Cancellation System Implementation

A stored-value I-Q cancellation system implemented in the RF section was chosen for the following reasons: the I-Q cancellation implemented with a wide-band hybrid 90° power splitter could be made to operate over an octave. A closed-loop cancellation system was not feasible because the magnitude and phase of the feedthrough signal are only determined after a scan through an FFT. Thus a stored value system had to be used. The cancellation system was implemented in the RF section in order to optimize the dynamic range of the system.

The core of the cancellation system consists of a bi-phase modulator used as a wideband phase-shifter and an attenuator. A diagram of the system is shown in Figure 5-9.

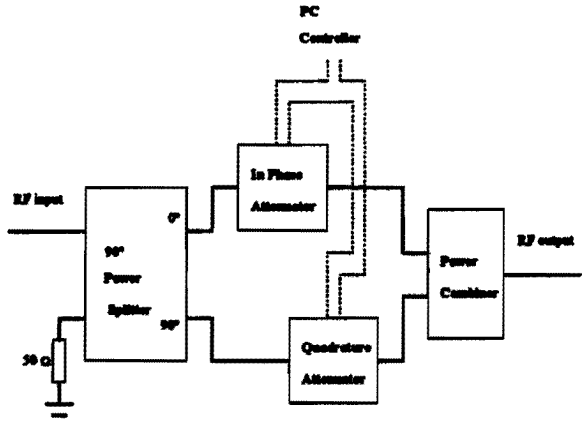

Figure 5-9: Block diagram of wide band phase shifter system

Conventional phase-shifters have a bandwidth of typically 10%. For the SFCW application, at least an octave bandwidth is required. The bi-phase modulator phase shifter operates as follows:

A portion of the transmit signal is coupled out and used as the input RF signal for the bi-phase modulator. This reference signal is applied to a wideband 90° power splitter. This bandwidth of the power splitter limits the bandwidth of the system. The power splitter used has a bandwidth from 330-660 MHz. The amplitude of the I and Q channels is controlled by electronic attenuators. These attenuators can attenuate the input signal with or without a 180° phase shift, depending on the sign of its control voltage. The two channels are then summed by a power combiner.

In order to simplify calibration, the bi-phase modulator was calibrated to operate

as a constant-magnitude phase-shifter. The magnitude of the cancellation vector is controlled by a PIN diode attenuator. The complete test setup is shown in Figure 5-10

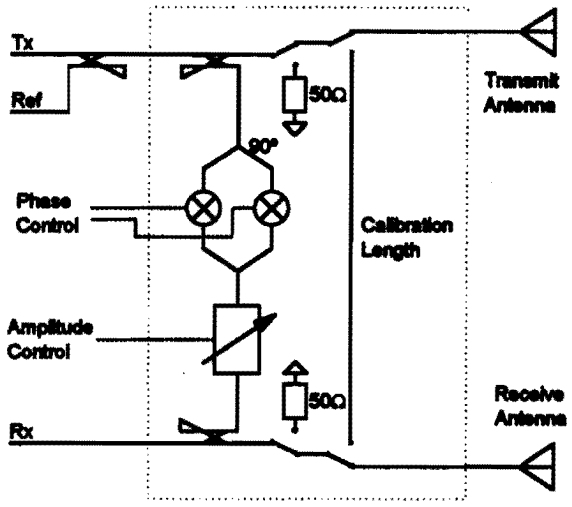

Figure 5-10: Complete Test System for signal cancellation unit

5.2.1 90° Power Splitter

The cancellation system has to operate over the full bandwidth of 300-1000 MHz. Thus transmission line or magnitude-phase systems were not feasible for this bandwidth of almost 2 octaves. The only design with octave bandwidths was the I-Q system. At the outset of the project, the maximum bandwidth possible for a 90° power splitter was 1 octave. It was thus decided to use two cancellation circuits to cover the whole bandwidth by splitting the bandwidth into the following two sections:

300-600 MHz using a QHF-2-.495GF by Merrimac
600-1000 MHz using a QHF-2-.750GF by Merrimac

Subsequent developments in 90° power splitter design have produced multi-octave components that cover the range 250-1000 MHz. Thus a single cancellation system could now be constructed using such a power splitter. For this reason, a single cancellation unit covering the band 300-600 MHz was thus constructed to prove the concept.

The quoted specifications of the power splitters are shown in Table 5.1. The power splitter was packaged in a stripline "sandwich" package and had to be mounted into the circuit board to ensure proper operation. Port 4 adjacent to the input port Port 1

Model Number	Frequency Range GHz	Isolation dB Min. Typ.	Insertion Loss(max) dB	Amplitude Balance pk-pk	Phase Quadrature
QHF-2-.495GF	.330-.660	25 30	3.25	1.0 dB	$90° \pm 2°$
QHF-2-.750GF	.500-1.00	25 30	3.25	1.0 dB	$90° \pm 2°$

Table 5.1: Power Splitters Specifications

was terminated in a 50Ω load. Port 2, the I output, and port 3, the Q output, were connected to the I and Q electronic attenuators respectively.

5.2.2 Electronic Attenuator

Two Mini-Circuits PAS-2 electronic attenuators were used to control the amplitudes of the I and Q channels. These attenuators could be driven by positive or negative voltages thus generating a 30 dB tuning range with or without 180° phase shift. The insertion loss was approximately 6 dB. The control voltage was applied to the control port via a bias circuit that acted like a 50Ω load above 1 MHz and like a series 500Ω resistor at low frequencies. Surface-mount blocking capacitors were used to block the DC bias of the attenuators.

A large coupling from the input to the output was observed at high attenuation settings and it was thus necessary to place a ground shield between these ports. Furthermore, ground shields consisting of copper-plated board were placed between the I and the Q channels to prevent cross-coupling.

5.2.3 Power Combiner

A Mini-Circuits PSC-2-4 power combiner was used to combine the I and Q channels into the output. The specifications for this power combiner can be seen in Table 5.2.3.

Model Number	Frequency Range MHz	Isolation dB Min. Typ.	Insertion Loss(max) dB	Amplitude Unbalance dB	Phase Unbalance deg
PSC-2-4	10-1000	20 25	3.2	0.4	±2°

Table 5.2: Power Combiner Specifications

5.2.4 Board Layout

The printed circuit board with a copper ground plane on the component side was used for the cancellation circuit. The board layout can be seen in Figure 5-11.

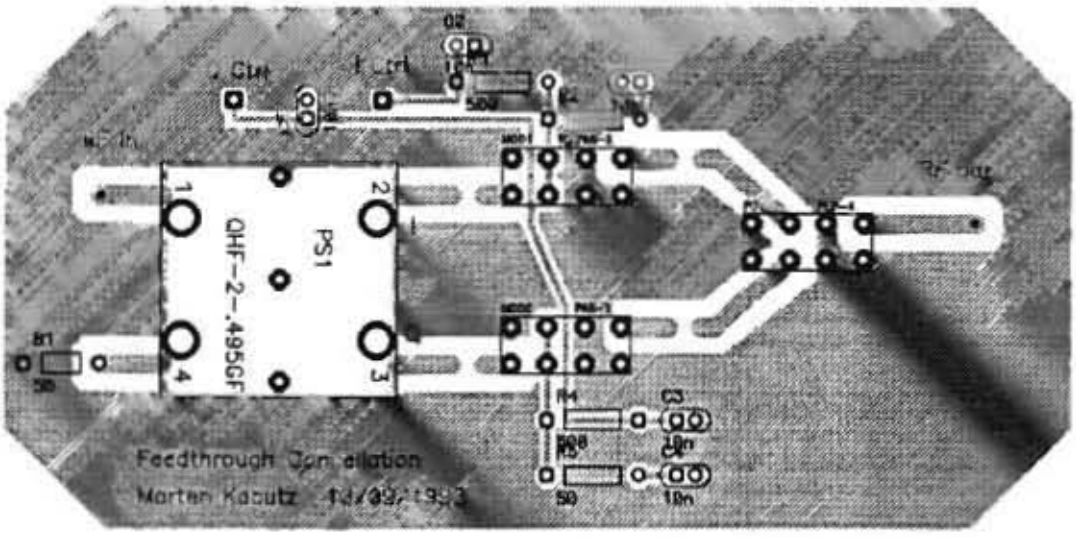

Figure 5-11: Cancellation System PCB

The I and Q channels were separated by a ground plane on the track side in order to reduce cross-coupling. Both channels were kept as straight as possible until the power combiner.

The rest of the cancellation system as shown in Figure 5-10 was also mounted inside the same case. Thus a power splitter, a switch to a 50Ω load and a switch to the 2 m calibration cable was included in both the transmit and the receive path. Simple SPDT mechanical switches were used. The isolation and insertion losses of these switches were acceptable for frequencies below 500 MHz. A full bandwidth system would thus require more sophisticated switches.

A photograph of the cancellation system showing the ground shields and the calibration

cable can be seen in Figure 5-12.

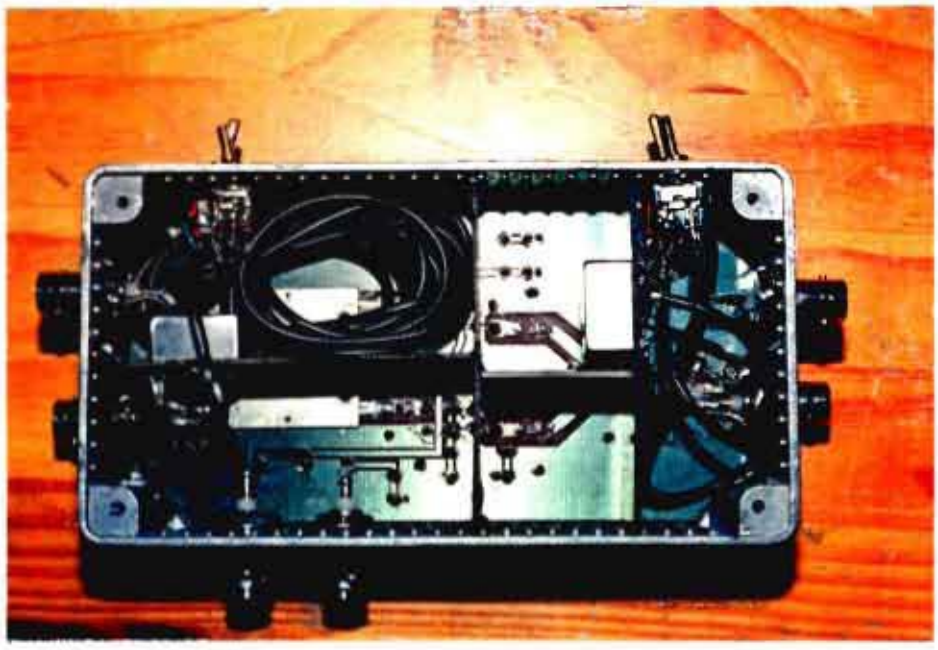

Figure 5-12: Photograph of Feedthrough Cancellation System

5.2.5 Calibration

It is necessary to determine the set of I and Q voltages to apply to generate the required phase shift from 0° to 360°. This is not a trivial task since the attenuators used in the phase shifter are highly non-linear and the external attenuator for amplitude control has a phase change with attenuation. There is also the added problem that the power combiner used to sum the radar signal with the generated cancellation vector has a phase unbalance, which must be taken into account.

The following calibration scheme per single frequency was implemented.

1. Using a boundary tracking algorithm, a set of I and Q voltages was obtained to produce a phase shift from 0 to 360° with a constant amplitude. The results of this calibration are shown in Figure 5-13 in terms of the phase error.
2. The frequency characteristic of a fixed length of cable was measured.
3. The error vector to cancel this calibration cable was determined using the I and Q calibrated phase data. The signal amplitude was set using the voltage controlled pin attenuator.

4. The cable was then adaptively nulled by adjusting the phase and amplitude determined from step 3. The difference between the phase and amplitude using the adaptive nulling and the phase and amplitude determined from step 3 is the phase and amplitude error introduced by the power splitters/combiners A and B in Figure 5-10.

This calibration is repeated for each of the step frequencies in the measurement bandwidth.

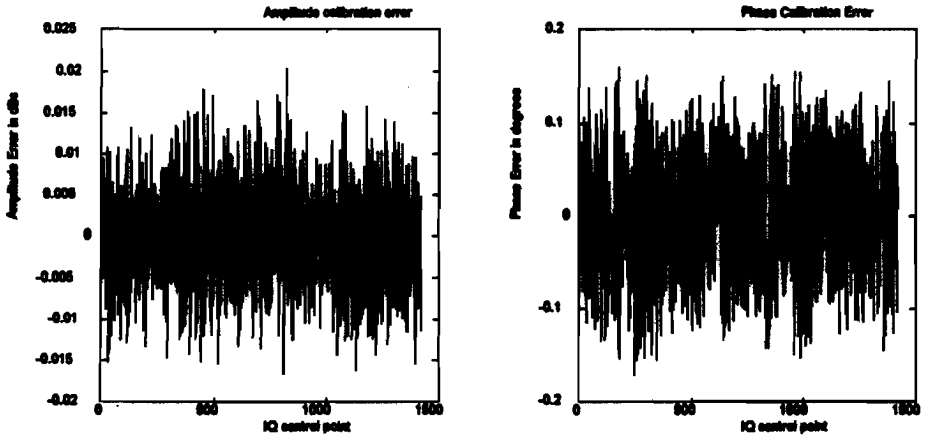

Figure 5-13: Calibration Amplitude and Phase Error for a single frequency (Results obtained in conjunction with Alan Langman [16])

5.2.6 Cancellation

The signal to be cancelled is determined from taking a measurement of the system without the cancellation circuit over a bandwidth required. From this signal, using an FFT or other target extraction method, the desired coupling vector is extracted. The set of I, Q and amplitude control voltages for each frequency is then determined from the calibration data. These are applied to the hardware at each frequency to cancel it from the measured signal.

5.3 Results

To prove the concept of this wide band cancellation system, a cable was cancelled over a 200 MHz bandwidth, from 300 MHz to 500 MHz. The phase and amplitude accuracy of the system was limited by the radar transmitter and receiver. For these results an HP8753 was used which has a phase accuracy of 0.3° and an amplitude accuracy 0.03 dB. The HP Network Analyzer was used to test the cancellation circuit to a greater degree of accuracy than would be possible using the transmitter and receiver systems. Using Equation 2.10 this gives an expected cancellation of better than 44 dB. The results of the calibration are shown in Figure 5-14.

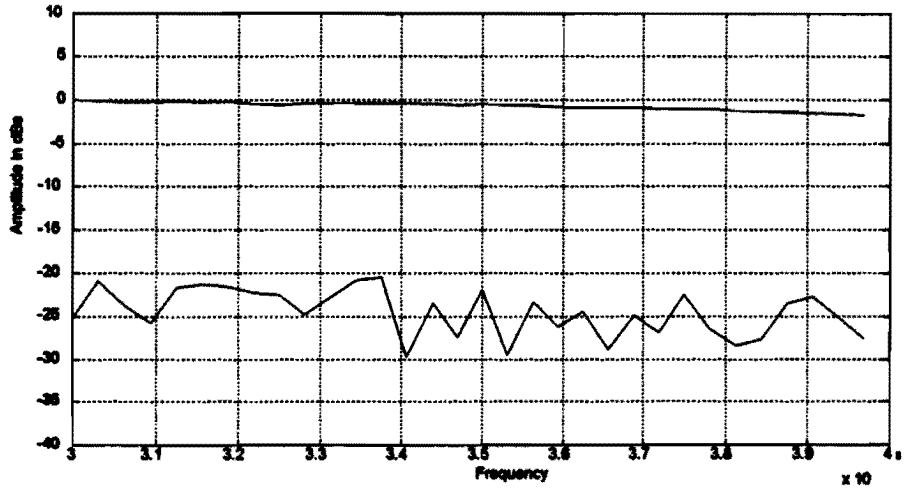

Figure 5-14: Cancellation of a cable (Results obtained in conjunction with Alan Langman [16])

The system was then used to remove the antenna coupling vector from a sub-surface image. The results are shown in Figures 5-15 and 5-16.

The concept of feedthrough cancellation has been proved by this study. A cable was cancelled out by applying a 180° shifted cancelling signal. A 20 dBV (40 dB) cancellation was obtained. The technique was then applied to a real sub-surface image by cancelling out the large antenna coupling vector. This method thus solves the problem of cancelling a single vector within a vector sum, thus improving on the conventional nulling techniques and thus the system dynamic range.

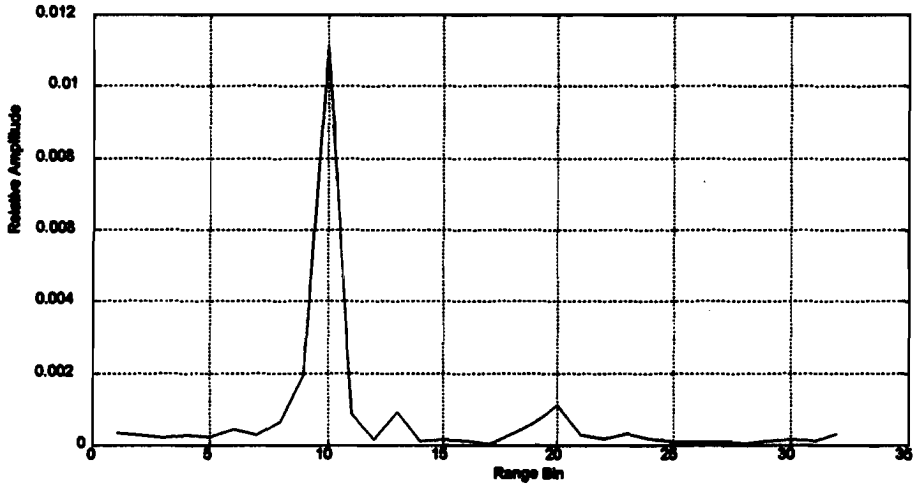

Figure 5-15: Sub-surface profile before cancellation of the antenna coupling(Results obtained in conjunction with Alan Langman [16])

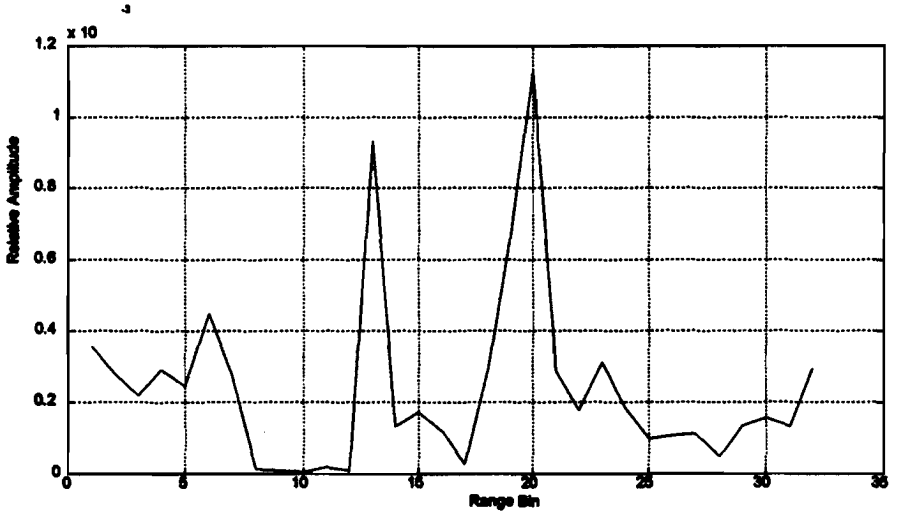

Figure 5-16: Sub-surface profile after cancellation of the antenna coupling(Results obtained in conjunction with Alan Langman [16])

Chapter 6

Results

The system was tested by measuring the response from various cable lengths and by measuring the response of a metal plate as it was moved towards the antennas. Finally, measurements of a shallow sand pit are presented.

6.1 Cable Length Measurement

Three cables if length 2m, 5m and 7m were used as dummy targets. The in-phase and quadrature components of the 2m cable are seen in Figure 6-1:

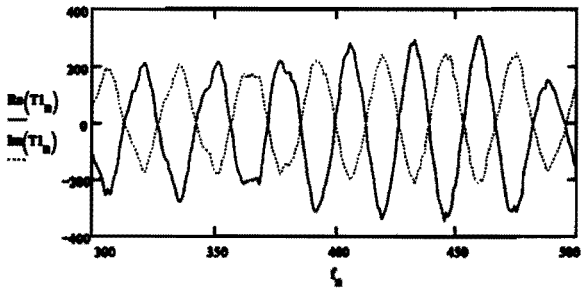

Figure 6-1: I and Q measurements for a 2m Cable target

The I and Q values are seen to be 180° out of phase with each other at all points. This is expected, since no information is modulated onto the phase of the IF in a double-sideband system. By taking the FFT's of both the I and the Q, and adding the magnitudes, the frequency plot was transformed to a distance plot shown in Figure 6-2.

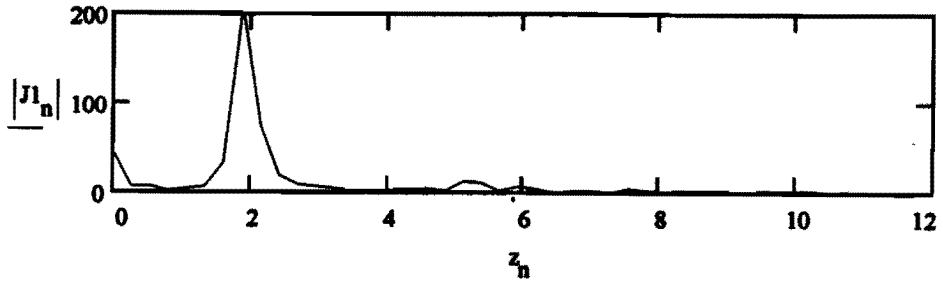

Figure 6-2: FFT distance measurements for a 2m Cable target

The response can be seen to be peak at approximately 2 m.

By the same procedure, the distance information was obtained for cables of length 5 m and 7 m. These are shown in Figures 6-3 and 6-4 respectively.

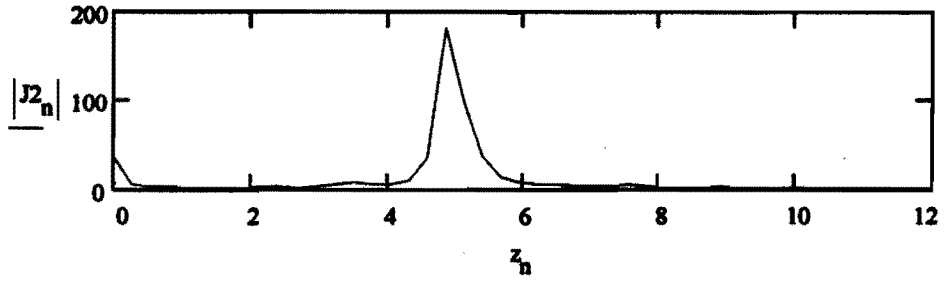

Figure 6-3: FFT distance measurements for a 5m Cable target

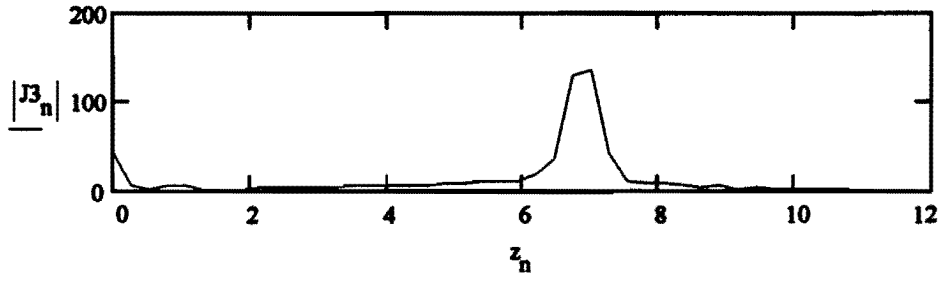

Figure 6-4: FFT distance measurements for a 7m Cable target

Superimposing the responses of the three cables (Figure 6-5), the lengths can be seen to be accurate within the resolution of 27 cm.

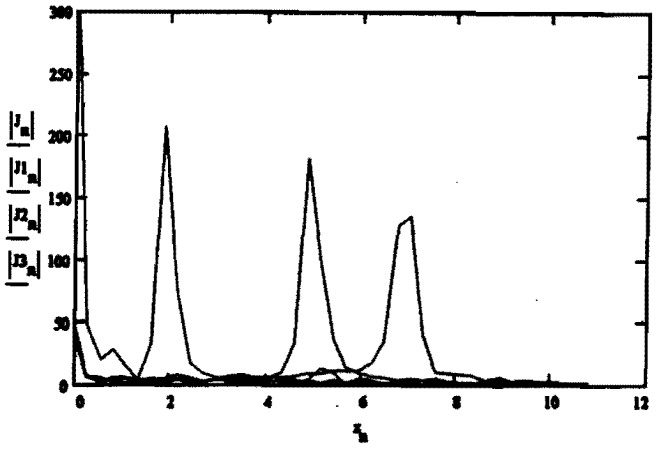

Figure 6-5: Distance measurements for all Cables

6.2 Plate Position Measurements

For the plate measurements, two cavity-backed spiral antenna were used to transmit and receive the signal. The two antennas were circularly polarized in opposite senses. A metal plate was moved towards the antennas starting from a distance of 3m and measuring at 2m and 1m. The measurements were taken in a laboratory so that a great deal of clutter was observed. The I-Q measurements and FFT magnitude plots for the plate a distance of 3 m from the antennas are shown in Figures 6-6 and 6-7.

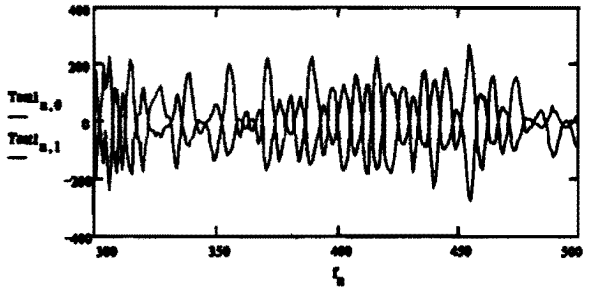

Figure 6-6: I and Q measurements for a Plate at 3m

The reflection from the plate can be seen clearly at approximately 3 m. A high clutter level can also be observed. The measurements are offset due to the length of cables to the antennas. Moving the plate to a distance of 2 m from the antenna resulted in the distance plot shown in Figure 6-8.

Here, the main reflection can be seen at a distance of 2 m, with a strong clutter component close to the target.

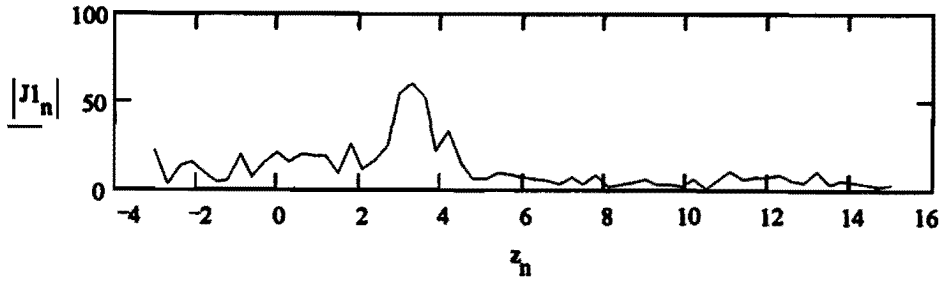

Figure 6-7: FFT distance measurements for a Plate target at 3m

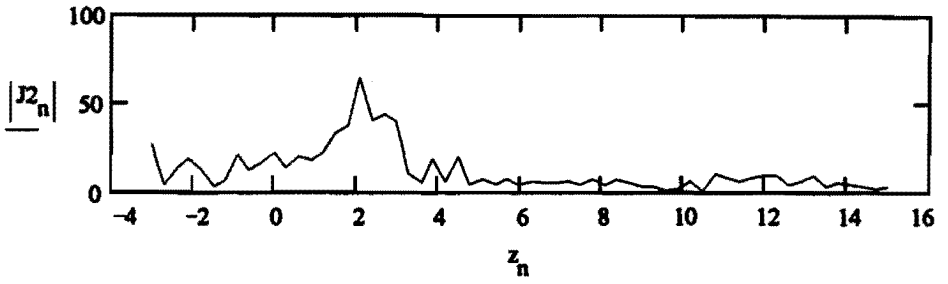

Figure 6-8: FFT distance measurements for a Plate target at 2m

Moving the plate to within 1 m of the antennas (shown in Figure 6-9) caused a large reflection as the plate covered a much greater percentage of the antenna bandwidths. The clutter level is of the same order as that of the plate at a further distance away.

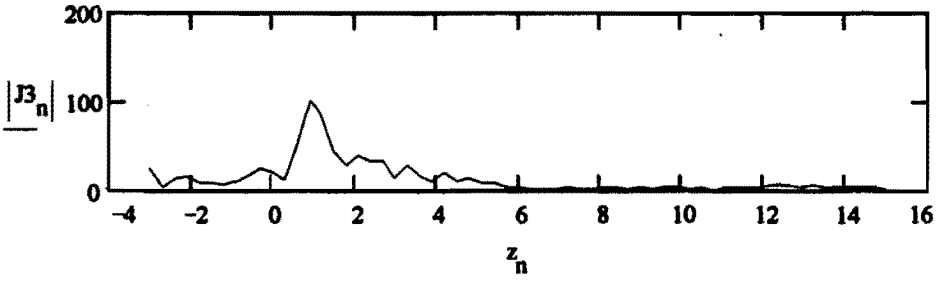

Figure 6-9: FFT distance measurements for a Plate target at 1m

The responses of the three plate positions are shown superimposed in Figure 6-10:

The response of the plate at 1 m can be seen to be greatly increased because of the wide beamwidth of the antennas (approximately 90°). The distances to the plates can be seen to be accurate to within the 30 cm resolution for this scan.

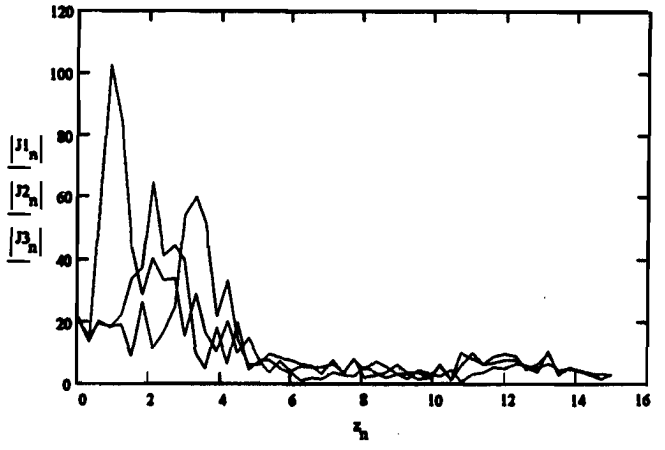

Figure 6-10: FFT distance measurements for a Plate targets at 1m, 2m, 3m

6.3 Sandpit Measurement

A shallow sandpit on a concrete floor was illuminated by using two cavity-backed spiral antennas. The response corrected for the offset caused by the cable length is shown in Figure 6-11.

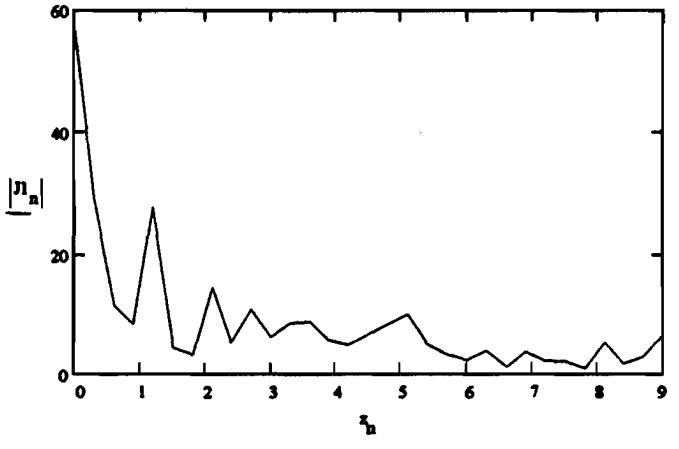

Figure 6-11: FFT distance measurements for a Sandpit depth 1m

A large coupling component can be observed at z=0. A large reflection at 1.2 m occurs at the approximate location of the expected sand/ground interface. Thus a concrete floor beneath 1 m of sand could be detected.

Chapter 7

Conclusions and Recommendations

Based on the findings of this report and the experience gained through the work, the following conclusions can be drawn:

- A UHF stepped frequency continuous wave ground penetrating radar was designed, constructed and found to operate satisfactorily. Several limitations due to the chosen designs were found and recommendations on an improved third generation system are given.
- A 300-1000 MHz CW transmitter using three switched VCOs was designed, constructed and tested. The transmitter provided an output power of +26 dBm over the bandwidth of 300 to 1000 MHz. The transmitter performance was degraded by two effects: frequency jitter and frequency step error. These effects reduced the effective time domain dynamic range to 45 dB. The free-running VCO design was thus found not to be suitable for high dynamic range measurements.
- A 300-1000 MHz CW receiver using a double-sideband single IF system was designed, constructed and tested. The dynamic range was measured to be 50 dB, which is less than desired. Improvements on the receiver design to increase the dynamic range are given in the recommendations.
- A 300-600 MHz feedthrough cancellation circuit was designed, constructed and found to cancel at least 40 dB of the feedthrough signal. The concept of feedthrough cancellation was thus proven. A second system to cover the 600-1000 MHz bandwidth was not constructed because recent advances in 90° power splitters made it

possible to construct a single cancellation system over the complete 300-1000 MHz bandwidth.

- The size of the system was kept small enough to fit onto the back of two cavity-backed spiral antennas. The voltage required for all the systems was kept to a standard +15 V which could be supplied through rechargeable batteries.
- The system was tested by measuring the lengths of cables and the distance to target plates. The measurement accuracy was found to be within the resolution and the dynamic range in the time domain was measured to be 42 dB. A concrete floor was detected under 1 m of sand.

Based on the findings of this report, the experience gained through the work and the above conclusions, recommendations on improvements on the system and future work are made. These recommendations should be used to optimize the system into a third generation SFCW GPR.

7.1 Transmitter Improvements

The transmitter performance was degraded by two effects: frequency jitter and frequency step error. These effects reduced the effective time domain dynamic range to 45 dB. Methods to reduce these frequency errors in the transmitter should be investigated.

Phase-locked loops should reduce the frequency step error and also the frequency jitter. Thus the phase-locked loop design should be investigated in detail.

The use and possible construction of low-cost frequency synthesizers should also be investigated.

7.2 Receiver Improvements

Recommendations on receiver improvements can be seen in the block diagram of a suggested improved receiver in Figure 7-1.

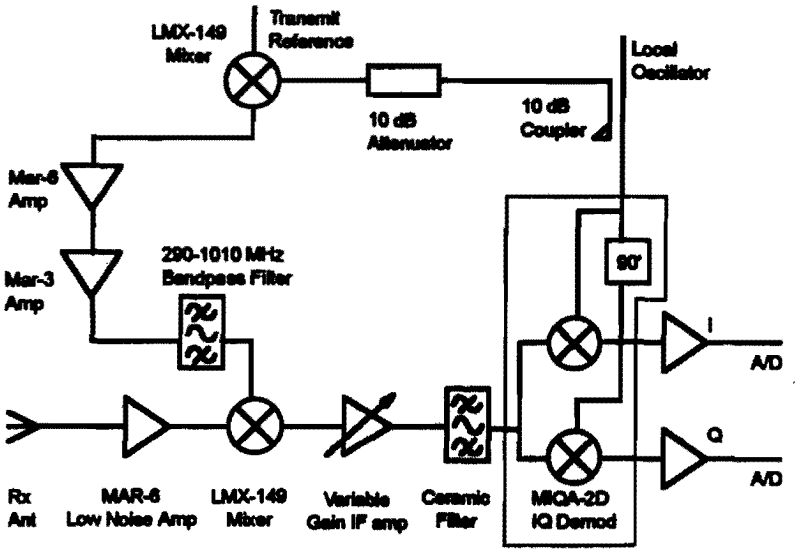

Figure 7-1: Block Diagram of Improved Receiver

The following improvements in the receiver design should be investigated:

- The feasibility of single-sideband system with I-Q detection in terms of bandwidth, cost and complexity should be investigated. Such a system would allow the full unambiguous range to be processed.
- Reducing the 10.7 MHz signal fed to the first mixer from 0 dBm to -10 dBm and increasing the gain of the mixer amplifier chain by 10 dB will reduce the level of unwanted products in the mixing signal from -30 dBc to -50 dBc.
- The necessity of a bandpass filter in the mixing signal path on the receiver performance should be investigated.
- A variable gain IF amplifier should be added into the IF path in order to optimize the dynamic range.
- An amplifier with a gain of 12.5 should be used to replace the instrumentation amplifier.
- The use of a DC logarithmic amplifier between the detector and the A/D converter should be investigated.

7.3 Cancellation Improvements

A single 300-1000 MHz cancellation system should be constructed using the present design with a multi-octave 90° phase splitter. This would improve on the initial design of covering the bandwidth with two cancellation circuits.

Methods of obtaining a greater degree of isolation between the I and Q channels should be investigated. Possible improvements could be achieved by the use of isolators around the bi-phase attenuators.

Linearized pin-diode attenuators are available to a high degree of attenuation linearity, simplifying control and calibration. Since pin-diodes cannot be used to switch the phase, four attenuators at 90° offsets would be required to control the cancellation vector. The relative merits of this configuration should be investigated.

7.4 Control and Data Handling Improvements

A dedicated microcontroller-based control unit should be constructed to replace the PC control of the system with a small dedicated unit which can be fitted onto the back of the antennas with the RF hardware.

A dedicated data capture unit should be constructed to replace the PC-74 card connected to a PC. This should also be fitted onto the antennas.

An optical fibre link from the data capture unit to the data storage, processing and visualization unit. This can be based on a PC or on a DSP system.

Bibliography

[1] Avantek, 3175 Bowers Avenue, Santa Clara, Ca 95051. *Solid State Microwave Components Product Guide*, 1986.

[2] P.D.L. Beasley, A.G. Stove, and B.J. Reits. Solving the Problems of a Single Antenna Frequency Modulated CW Radar. In *IEEE International Radar Conference*, pages 391–395, January 1990.

[3] Arun K. Bhattacharyya. Effects of ground plane and dielectric truncations on the efficiency of a printed structure. *IEEE Trans on Antennas and Propagation*, 39(3):303–308, March 1991.

[4] J.L. Brown. On Quadrature Sampling of Bandpass Signals. *IEEE Trans on Aerospace and Electronic Systems*, 15(3):366–371, May 1979.

[5] J.C. Fowler, S.D. Hale, and R.T. Houck. *Coal Mine Hazard Detection Using Synthetic Pulse Radar*. RnMines OFR 79-81, ENSCO Inc., US Bureau of Mines Contract H0292925, January 1981.

[6] Alois P. Freundorfer and Keigo Iizuka. Detection of Nonmetallic Buried Objects by a Step Frequency Radar. In *Proceedings of the IEEE*, volume 71, pages 277–279. IEEE Proceedings, February 1983.

[7] A.P. Freundorfer. *Step Frequency Radar*. PhD thesis, University of Toronto, July 1989.

[8] O.D. Grace and S.P. Pitt. Quadrature Sampling of High-frequency Waveforms. *The Journal of the Acoustical Society of America*, 44(5):1453–1454, March 1968.

[9] J D Harmer and W S O'Hare. Some Advances in CW Radar Techniques. *IRE 5th MIL-E-CON Record*, loud:311–323, 1969.

[10] Hewlett Packard. *Phase Noise Characterization of Microwave Oscillators*, March 1984.

[11] Hipp. Soil Electromagnetic Parameters as Functions of Frequency, Soil Density, and Soil Moisture. In *Proceedings of the IEEE*, volume 62, pages 98–103. IEEE Proceedings, January 74.

[12] P. Hoekstra and A. Delaney. Dielectric Properties of Soils and UHF and Microwave Frequencies . *Journal of Geophysical Research*, 79(11):1699–1708, April 1974.

[13] S.A. Hovanessian. *Radar System Design and Analysis* . Artech House, Norwood, MA, January 1984.

[14] Keigo Iizuka, Ogura Hisanoa, and N Van-Khai. A hologram matrix radar. In *IEEE Proceedings*, pages 1493–1504, October 1976.

[15] Keigo Iizuka, Kam Hung Wu, Hirotaka Mori, Hisanao Ogura, Van-Khai Nguyen, and Alois P. Freundorfer. Step-frequency radar. *J. Appl. Phys.*, 56(9):2572–2583, November 1984.

[16] M.R. Inggs and ADM Garvin. Stepped-frequency continuous wave ground penetrating radar images. volume AP/MTTS-91, pages 178–183, Halfway House, South Africa, August 1991. IEEE/SAIEE AP/MTT Symposium.

[17] M.R. Inggs, M. Kabutz, and A. Langman. Hardware cancellation of the direct coupling in a stepped cw ground penetrating radar. In *Proceedings of the 1994 International Geoscience & Remote Sensing Symposium (IGARSS '94)*, volume 4, pages 2505–2507, Pasadena, USA, August 94. IGARSS '94.

[18] M.R. Inggs, A. Langman, and M.H. Kabutz. A summary of feedthrough cancellation techniques for cw radar. SAIEE Conf. Antennas and Propagat., 93.

[19] Peter S. Kao. Automated Step-Frequency Radar Cross-Section Measurements . *CALIFORNIA SCIENTIFIC SOFTWARE*, pages 237–239.

[20] A. Kohlenberg. Exact Interpolation of Band-limited Functions. *Journal of Applied Physics*, 24(12):1432–1436, December 1953.

[21] Merrimac, 41 Fairfield Place, West Caldwell, N.J. 07006. *RF and Microwave Processing M-94*, 1994.

[22] Mini-Circuits Division of Scientific Components, 13 Neptune Avenue, Brooklyn, NY 11235. *RF/IF Designer's Handbook*, 92/93.

[23] Paul Horowitz and Winfield Hill. *The Art of Electronics* . CAMBRIDGE UNIVERSITY PRESS, 1989.

[24] Merril I Skolnik. *Introduction to Radar Systems, 2nd Edition.* McGraw-Hill Book Company, New York, January 1980.

[25] S. Uratsuka, K. Okamoto, H. Mineno, and S. Mae. Step Frequency Radar Experiments on the Antartica Sea Ice . In *Proceedings of the 1988 International Geoscience & Remote Sensing Symposium (IGARSS '88)*, pages 1703–1706, Edinburgh, Scotland, September 1988. IGARSS '88.

[26] Yoshio Yamaguchi, Yasuichi Maruyama, Atushi Kawakami, Masakazu Sengoku, and Takeo Abe. Detection of Objects Buried in Wet Snowpack by an FM-CW Radar. *IEEE Trans on Geosc. and Remote Sensing*, 29(2):201–208, March 1991.

Appendix A

Receiver Calculations

A.1 Single- and Double Sideband Systems

The receiver can be used as either a single- or a double sideband system. In a single sideband system only one sideband of the mixing signal $f_{Tx} \pm f_{LO}$ is used. A double sideband system uses both $f_{Tx} + f_{LO}$ and $f_{Tx} - f_{LO}$ sidebands. The actual measurements that are taken with these two types of systems are markedly different. For a transmit signal of $V_t sin(w_t t)$, and an IF signal of $V_{IF} sin(w_{IF} t)$, the output of the first mixer is

$$V_{mix} = \frac{V_{LO}}{2L_{mix}}[cos((w_t - w_{IF})t + \theta_{e1}) - cos((w_t + w_{IF})t + \theta_{e1})] \qquad (A.1)$$

where L_{mix} is the mixer loss and θ_{e1} is the phase shift added by the signal path of the reference signal. In this case the reference signal f_{Tx} was used to drive the mixer and thus the output is independent of the reference signal level.

A.1.1 Single Sideband System

For a single-sideband system using a filtering system, one of the sidebands is rejected and the other used to drive the receiver mixer. If, for example, the upper sideband is used, the signal driving the receiver mixer will be:

$$V_{mix} = -\frac{V_{LO}}{2L_{mix}} cos((w_t + w_{IF})t + \theta_{e1} + \theta_{e2}) \quad (A.2)$$

where θ_{e2} is the phase shift due to the signal path from the first mixer to the receive mixer. The received signal will be of the form $V_r sin(w_t t + \theta_r)$ where V_r is a fraction of V_t which can be calculated by the radar equation and θ_r is the phase shift due to the propagation path to the target and back. The output of the receiver mixer will be:

$$V_{IF} = -\frac{V_r}{2L_{mix}}[sin(-w_{IF}t + \theta_r - \theta_{e1} - \theta_{e2}) + sin((2w_t + w_{IF})t + \theta_r + \theta_{e1} + \theta_{e2})] \quad (A.3)$$

Band-pass filtering this signal to the IF frequency yields:

$$V_{IF} = \frac{V_r}{2L_{mix}}[sin((w_{IF})t - \theta_r + \theta_{e1} + \theta_{e2})] \quad (A.4)$$

Detecting the IF in magnitude-phase or I-Q yields the complex signal information by which the time-domain plot can be obtained through the complex Fast Fourier transform. If a SSB mixer is used, the rejected sideband energy is reflected onto the wanted sideband resulting in a 3 dB improvement over a filtering system.

A.1.2 Double-Sideband System

In a double-sideband system, both sidebands of the first mixer output are used to drive the receiver mixer. Thus the driving signal is:

$$V_{mix} = \frac{V_{LO}}{2L_{mix}}[cos((w_t - w_{IF})t + \theta_{e1} + \theta e2) - cos((w_t + w_{IF})t + \theta_{e1} + \theta e2)] \quad (A.5)$$

where $\theta e2$ is the phase shift due to the signal path from the first mixer to the receiver mixer. The received signal is $V_r sin(w_t t + \theta_r)$ where V_r and θ_r are the magnitude and phase shift due to the propagation to and from the target. The IF signal is thus:

$$V_{IF} = \frac{V_r}{2L_{mix}}[sin(w_{IF}t + \theta_r - \theta_{e1} - \theta_{e2}) + sin((2w_t - w_{IF})t + \theta_r + \theta_{e1} + \theta_{e2}) \\ -sin(-w_{IF}t + \theta_r - \theta_{e1} - \theta_{e2}) + sin((2w_t + w_{IF})t + \theta_r + \theta_{e1} + \theta_{e2})] \quad (A.6)$$

Bandpass filtering this signal to the IF frequency yields:

$$V_{IF} = \frac{V_r}{2L_{mix}}[sin(w_{IF}t + \theta_r - \theta_{e1} - \theta_{e2}) - sin(-w_{IF}t + \theta_r - \theta_{e1} - \theta_{e2})] \quad (A.7)$$

This can be reduced to:

$$V_{IF} = \frac{V_r}{L_{mix}}[cos(\theta_r - \theta_{e1} - \theta_{e2})sin(w_{IF}t)] \quad (A.8)$$

Thus both the magnitude and phase of the received signal are modulated onto the amplitude of the IF and there is no information in the IF phase.

A.2 Power and Noise Budget Calculations

A.2.1 According to specifications

Capitals = dB, small = linear

$Tx := 10 \cdot dBm$ Transmit Power into Receiver

$Lo := 0 \cdot dBm$ Local Oscillator Power

$L_{mix} := 7 \cdot dB$ Mixer Conversion Loss

$G_{mar4} := 8 \cdot dB$ MAR-4 gain

$G_{mar6} := 18 \cdot dB$ MAR-6 gain

$g_{mar4} := lin(G_{mar4})$ $g_{mar4} = 6.31$

$g_{mar6} := lin(G_{mar6})$ $g_{mar6} = 63.096$

LO Level at receiver mixer:

$Lo := Lo - L_{mix} + G_{mar4} + G_{mar4}$

$Lo = 9 \cdot dBm$

Received Signal

$k := 1.38 \cdot 10^{-23}$

$T := 290$

$B := 200000$ 200 kHz Bandwidth

$n := 4 \cdot k \cdot T \cdot B \cdot 10^{3}$ $n = 3.202 \cdot 10^{-12} \cdot mW$ Antenna Noise Power (in mW)

$n := 2 \cdot n$ $n = 6.403 \cdot 10^{-12} \cdot mW$ Image Noise

$N := db(n)$ $N = -111.936 \cdot dBm$ Antenna Noise Power (in dBm)

$G_{conn} := -1 \cdot dB$ Connector and cable loss

$g_{conn} := lin(G_{conn})$ $g_{conn} = 0.794$

$nf_{conn} := \frac{1}{g_{conn}}$ $nf_{conn} = 1.259$ Connector and cable noise figure

$NF_{mar6} := 3 \cdot dB$ Preamplifier Noise Figure

$nf_{mar6} := lin(NF_{mar6})$ $nf_{mar6} = 1.995$

$g_{mix} := lin(-L_{mix})$ $g_{mix} = 0.2$ Mixer gain

$NF_{mix} := L_{mix} + 0.5$ Mixer Noise Figure

$nf_{mix} := lin(NF_{mix})$ $nf_{mix} = 5.623$

$G_{IFamp} := 20 \cdot dB$ IF amplifier gain

$g_{IFamp} := lin(G_{IFamp})$ $g_{IFamp} = 100$

$nf_{IFamp} := 10$ $nf_{IFamp} = 10$ IF amplifier Noise Figure

$G_{IFfilter} := -10 \cdot dB$ IF filter gain

$g_{IFfilter} := lin(G_{IFfilter})$ $g_{IFfilter} = 0.1$

$nf_{IFfilter} := \frac{1}{g_{IFfilter}}$ $nf_{IFfilter} = 10$ IF filter Noise Figure

$$nf := nf_{conn} + \frac{nf_{mar6} - 1}{g_{conn}} + \frac{nf_{mix} - 1}{g_{mar6}} + \frac{nf_{IFamp} - 1}{g_{mar6} \cdot g_{mix}} + \frac{nf_{IFfilter} - 1}{g_{mar6} \cdot g_{mix} \cdot g_{IFamp}}$$

$nf = 3.307$ **System Noise Figure**

$n_{eq} := n \cdot nf$ $n_{eq} = 2.118 \cdot 10^{-11} \cdot mW$ Equivalent Input Noise Power

$N_{eq} := db(n_{eq})$ $N_{eq} = -106.741 \cdot dBm$

$S_{in\_max} := -20 \cdot dBm$ Maximum input signal

$SNR_{min} := 10 \cdot dB$ Minimum Signal to Noise Ratio

$S_{in\_min} := N_{eq} + SNR_{min}$ Minimum Input Signal

$Dynamic\_Range := S_{in\_max} - S_{in\_min}$

$Dynamic\_Range = 76.741 \cdot dB$

A typical target will be approximately 20 dB below the coupling level. Thus if the coupling signal is situated exactly at the top end of the dynamic range, the resultant effective dynamic range will be 57 dB. However, since the coupling level is not known exactly for all situations, the real effective dynamic range will be even less.

$L_{ant\_face} := 12 \cdot dB$ Tx-Rx Antenna loss when facing

$L_{ant} := 30 \cdot dB$ Coupling level

Maximum Transmit Power for no saturation:

$S_{out\_max} := S_{in\_max} + L_{ant}$

$S_{out\_max} = 10 \cdot dBm$ Antennas looking into the ground

$S_{out\_max} := S_{in\_max} + L_{ant\_face}$

$S_{out\_max} = -8 \cdot dBm$ Antennas are facing each other

Maximum Transmit Power for no damage:

$S_{in\_max} := 20 \cdot dBm$ Maximum Input Power when transmitting
(Max Input (no damage) = +20 dBm)

$S_{out\_max} := S_{in\_max} + L_{ant}$

$S_{out\_max} = 50 \cdot dBm$ Antennas looking into the ground

$S_{out\_max} := S_{in\_max} + L_{ant\_face}$

$S_{out\_max} = 32 \cdot dBm$ Antennas are facing each other

A.2.2 Measuring Parameters at 300 MHz

Capitals = dB, small = linear

$Tx := 10 \cdot dBm$ Transmit Power into Receiver

$Lo := 0 \cdot dBm$ Local Oscillator Power

$L_{mix} := 7.7 \cdot dB$ Mixer Conversion Loss

$G_{mar4} := 7.5 \cdot dB$ MAR-4 gain

$G_{mar6} := 17 \cdot dB$ MAR-6 gain

$g_{mar4} := lin(G_{mar4})$ $g_{mar4} = 5.623$

$g_{mar6} := lin(G_{mar6})$ $g_{mar6} = 50.119$

LO Level at receiver mixer:

$Lo := Lo - L_{mix} + G_{mar4} + G_{mar4}$

$Lo = 7.3 \cdot dBm$

Received Signal

$k := 1.38 \cdot 10^{-23}$

$T := 290$

$B := 200000$ 200 kHz Bandwidth

$n := 4 \cdot k \cdot T \cdot B \cdot 10^{3}$ $n = 3.202 \cdot 10^{-12} \cdot mW$ Antenna Noise Power (in mW)

$n := 2 \cdot n$ $n = 6.403 \cdot 10^{-12} \cdot mW$ Image Noise

$N := db(n)$ $N = -111.936 \cdot dBm$ Antenna Noise Power (in dBm)

$G_{conn} := -1 \cdot dB$ Connector and cable loss

$g_{conn} := lin(G_{conn})$ $g_{conn} = 0.794$

$nf_{conn} := \frac{1}{g_{conn}}$ $nf_{conn} = 1.259$ Connector and cable noise figure

$NF_{mar6} := 3 \cdot dB$ Preamplifier Noise Figure

$nf_{mar6} := lin(NF_{mar6})$ $nf_{mar6} = 1.995$

$g_{mix} := lin(-L_{mix})$ $g_{mix} = 0.17$ Mixer gain

$NF_{mix} := L_{mix} + 0.5$ Mixer Noise Figure

$nf_{mix} := lin(NF_{mix})$ $nf_{mix} = 6.607$

$G_{IFamp} := 20 \cdot dB$ IF amplifier gain

$g_{IFamp} := lin(G_{IFamp})$ $g_{IFamp} = 100$

$nf_{IFamp} := 10$ $nf_{IFamp} = 10$ IF amplifier Noise Figure

$G_{IFfilter} := -10 \cdot dB$ IF filter gain

$g_{IFfilter} := lin(G_{IFfilter})$ $g_{IFfilter} = 0.1$

$nf_{IFfilter} := \frac{1}{g_{IFfilter}}$ $nf_{IFfilter} = 10$ IF filter Noise Figure

$$nf := nf_{conn} + \frac{nf_{mar6} - 1}{g_{conn}} + \frac{nf_{mix} - 1}{g_{mar6}} + \frac{nf_{IFamp} - 1}{g_{mar6} \cdot g_{mix}} + \frac{nf_{IFfilter} - 1}{g_{mar6} \cdot g_{mix} \cdot g_{IFamp}}$$

$nf = 3.692$ **System Noise Figure**

$n_{eq} := n \cdot nf$ $n_{eq} = 2.364 \cdot 10^{-11} \cdot mW$ Equivalent Input Noise Power

$N_{eq} := db(n_{eq})$ $N_{eq} = -106.264 \cdot dBm$

$S_{in\_max} := -20 \cdot dBm$ Maximum input signal

$SNR_{min} := 10 \cdot dB$ Minimum Signal to Noise Ratio

$S_{in\_min} := N_{eq} + SNR_{min}$ Minimum Input Signal

$Dynamic\_Range := S_{in\_max} - S_{in\_min}$

$Dynamic\_Range = 76.264 \cdot dB$

A typical target will be approximately 20 dB below the coupling level. Thus if the coupling signal is situated exactly at the top end of the dynamic range, the resultant effective dynamic range will be 56 dB. However, since the coupling level is not known exactly for all situations, the real effective dynamic range will be even less.

$L_{ant\_face} := 12 \cdot dB$ Tx-Rx Antenna loss when facing

$L_{ant} := 30 \cdot dB$ Coupling level

Maximum Transmit Power for no saturation:

$S_{out\_max} := S_{in\_max} + L_{ant}$

$S_{out\_max} = 10 \cdot dBm$ Antennas looking into the ground

$S_{out\_max} := S_{in\_max} + L_{ant\_face}$

$S_{out\_max} = -8 \cdot dBm$ Antennas are facing each other

Maximum Transmit Power for no damage:

$S_{in\_max} := 20 \cdot dBm$ Maximum Input Power when transmitting (Max Input (no damage) = +20 dBm)

$S_{out\_max} := S_{in\_max} + L_{ant}$

$S_{out\_max} = 50 \cdot dBm$ Antennas looking into the ground

$S_{out\_max} := S_{in\_max} + L_{ant\_face}$

$S_{out\_max} = 32 \cdot dBm$ Antennas are facing each other

A.2.3 Measuring Parameters at 1000 MHz

Capitals = dB, small = linear

$Tx := 10 \cdot dBm$ Transmit Power into Receiver

$Lo := 0 \cdot dBm$ Local Oscillator Power

$L_{mix} := 9 \cdot dB$ Mixer Conversion Loss

$G_{mar4} := 5.5 \cdot dB$ MAR-4 gain

$G_{mar6} := 12.2 \cdot dB$ MAR-6 gain

$g_{mar4} := lin(G_{mar4})$ $g_{mar4} = 3.548$

$g_{mar6} := lin(G_{mar6})$ $g_{mar6} = 16.596$

LO Level at receiver mixer:

$Lo := Lo - L_{mix} + G_{mar4} + G_{mar4}$

$Lo = 2 \cdot dBm$

Received Signal

$k := 1.38 \cdot 10^{-23}$

$T := 290$

$B := 200000$ 200 kHz Bandwidth

$n := 4 \cdot k \cdot T \cdot B \cdot 10^{3}$ $n = 3.202 \cdot 10^{-12} \cdot mW$ Antenna Noise Power (in mW)

$n := 2 \cdot n$ $n = 6.403 \cdot 10^{-12} \cdot mW$ Image Noise

$N := db(n)$ $N = -111.936 \cdot dBm$ Antenna Noise Power (in dBm)

$G_{conn} := -1 \cdot dB$ Connector and cable loss

$g_{conn} := lin(G_{conn})$ $g_{conn} = 0.794$

$nf_{conn} := \frac{1}{g_{conn}}$ $nf_{conn} = 1.259$ Connector and cable noise figure

$NF_{mar6} := 3 \cdot dB$ Preamplifier Noise Figure

$nf_{mar6} := lin(NF_{mar6})$ $nf_{mar6} = 1.995$

$g_{mix} := lin(-L_{mix})$ $g_{mix} = 0.126$ Mixer gain

$NF_{mix} := L_{mix} + 0.5$ Mixer Noise Figure

$nf_{mix} := lin(NF_{mix})$ $nf_{mix} = 8.913$

$G_{IFamp} := 20 \cdot dB$ IF amplifier gain

$g_{IFamp} := lin(G_{IFamp})$ $g_{IFamp} = 100$

$nf_{IFamp} := 10$ $nf_{IFamp} = 10$ IF amplifier Noise Figure

$G_{IFfilter} := -10 \cdot dB$ IF filter gain

$g_{IFfilter} := lin(G_{IFfilter})$ $g_{IFfilter} = 0.1$

$nf_{IFfilter} := \frac{1}{g_{IFfilter}}$ $nf_{IFfilter} = 10$ IF filter Noise Figure

$$nf := nf_{conn} + \frac{nf_{mar6} - 1}{g_{conn}} + \frac{nf_{mix} - 1}{g_{mar6}} + \frac{nf_{IFamp} - 1}{g_{mar6} \cdot g_{mix}} + \frac{nf_{IFfilter} - 1}{g_{mar6} \cdot g_{mix} \cdot g_{IFamp}}$$

$nf = 7.339$ **System Noise Figure**

$n_{eq} := n \cdot nf$ $n_{eq} = 4.7 \cdot 10^{-11} \cdot mW$ Equivalent Input Noise Power

$N_{eq} := db(n_{eq})$ $N_{eq} = -103.279 \cdot dBm$

$S_{in\_max} := -20 \cdot dBm$ Maximum input signal

$SNR_{min} := 10 \cdot dB$ Minimum Signal to Noise Ratio

$S_{in\_min} := N_{eq} + SNR_{min}$ Minimum Input Signal

$Dynamic\_Range := S_{in\_max} - S_{in\_min}$

$Dynamic\_Range = 73.279 \cdot dB$

A typical target will be approximately 20 dB below the coupling level. Thus if the coupling signal is situated exactly at the top end of the dynamic range, the resultant effective dynamic range will be 53 dB. However, since the coupling level is not known exactly for all situations, the real effective dynamic range will be even less.

$L_{ant\_face} := 12 \cdot dB$ Tx-Rx Antenna loss when facing

$L_{ant} := 30 \cdot dB$ Coupling level

Maximum Transmit Power for no saturation:

$S_{out\_max} := S_{in\_max} + L_{ant}$

$S_{out\_max} = 10 \cdot dBm$ Antennas looking into the ground

$S_{out\_max} := S_{in\_max} + L_{ant\_face}$

$S_{out\_max} = -8 \cdot dBm$ Antennas are facing each other

Maximum Transmit Power for no damage:

$S_{in\_max} := 20 \cdot dBm$ Maximum Input Power when transmitting (Max Input (no damage) = +20 dBm)

$S_{out\_max} := S_{in\_max} + L_{ant}$

$S_{out\_max} = 50 \cdot dBm$ Antennas looking into the ground

$S_{out\_max} := S_{in\_max} + L_{ant\_face}$

$S_{out\_max} = 32 \cdot dBm$ Antennas are facing each other